National Library of Canada
Bibliothèque nationale du Canada

Canadian Theses Service
Service des thèses canadiennes

Ottawa, Canada
K1A 0N4

NOTICE

The quality of this microform is heavily dependent upon the quality of the original thesis submitted for microfilming. Every effort has been made to ensure the highest quality of reproduction possible.

If pages are missing, contact the university which granted the degree.

Some pages may have indistinct print especially if the original pages were typed with a poor typewriter ribbon or if the university sent us an inferior photocopy.

Previously copyrighted materials (journal articles, published tests, etc.) are not filmed.

Reproduction in full or in part of this microform is governed by the Canadian Copyright Act, R.S.C. 1970, c. C-30.

AVIS

La qualité de cette microforme dépend grandement de la qualité de la thèse soumise au microfilmage. Nous avons tout fait pour assurer une qualité supérieure de reproduction.

S'il manque des pages, veuillez communiquer avec l'université qui a conféré le grade.

La qualité d'impression de certaines pages peut laisser à désirer, surtout si les pages originales ont été dactylographiées à l'aide d'un ruban usé ou si l'université nous a fait parvenir une photocopie de qualité inférieure.

Les documents qui font déjà l'objet d'un droit d'auteur (articles de revue, tests publiés, etc.) ne sont pas microfilmés.

La reproduction, même partielle, de cette microforme est soumise à la Loi canadienne sur le droit d'auteur, SRC 1970, c. C-30.

NL-339 (r. 88/04)

Canada

UNIVERSITY OF ALBERTA

A SUB-OPTIMAL AMPLITUDE CONTROL SYSTEM FOR A HARMONIC OSCILLATOR

BY

LUNDY TAYLOR

A THESIS

SUBMITTED TO THE FACULTY OF GRADUATE STUDIES AND RESEARCH

IN PARTIAL FULFILMENT OF THE REQUIREMENTS FOR THE DEGREE

OF MASTER OF SCIENCE

DEPARTMENT OF ELECTRICAL ENGINEERING

EDMONTON, ALBERTA

SPRING 1988

Permission has been granted to the National Library of Canada to microfilm this thesis and to lend or sell copies of the film.

The author (copyright owner) has reserved other publication rights, and neither the thesis nor extensive extracts from it may be printed or otherwise reproduced without his/her written permission.

L'autorisation a été accordée à la Bibliothèque nationale du Canada de microfilmer cette thèse et de prêter ou de vendre des exemplaires du film.

L'auteur (titulaire du droit d'auteur) se réserve les autres droits de publication; ni la thèse ni de longs extraits de celle-ci ne doivent être imprimés ou autrement reproduits sans son autorisation écrite.

ISBN 0-315-42829-5

THE UNIVERSITY OF ALBERTA

RELEASE FORM

NAME OF AUTHOR: LUNDY TAYLOR

TITLE OF THESIS: SUB-OPTIMAL AMPLITUDE CONTROL SYSTEM FOR A HARMONIC OSCILLATOR

DEGREE: MASTER OF SCIENCE

YEAR THIS DEGREE GRANTED: 1988

Permission is hereby granted to the UNIVERSITY OF ALBERTA LIBRARY to reproduce single copies of this thesis and to lend or sell such copies for private, scholarly or scientific research purposes only.

The author reserves other publication rights, and neither the thesis nor extensive extracts from it may be printed or otherwise reproduced without the author's written permission.

Lundy Taylor

5311 105A Ave.

Edmonton, Alberta

Date: Apr 22/88

THE UNIVERSITY OF ALBERTA

FACULTY OF GRADUATE STUDIES AND RESEARCH

The undersigned certify that they have read, and recommend to the Faculty of Graduate Studies and Research for acceptance, a thesis entitled

A Sub-Optimal Amplitude Control System

for a Harmonic Oscillator

submitted by Lundy Taylor

in partial fulfilment of the requirements for the degree of Master of Science

I D Lawrey
.....
(Supervisor)

R. E. Rink
.....

John W. Manke
.....

.....

Date: March 28, 1988

ABSTRACT

Optimal control theory was used to design an amplitude control system for a quadrature phase oscillator. Low distortion and fast settling time are important specifications of amplitude control systems; however, these criterion are normally contradictory. The approach discussed here eliminates the problem by designing two separate control systems, each of which has been optimized for the appropriate design goal. The complexity of the solution forces a sub-optimal implementation for which a circuit has been built and performance parameters measured. The THD obtained is better than -60dB and the settling time is better than half the period of oscillation.

TABLE OF CONTENTS

CHAPTER		PAGE
1	THE PROBLEM OF AMPLITUDE CONTROL	1
1.0	THE STRUCTURE OF AMPLITUDE CONTROL SYSTEMS	1
1.1	LITERATURE SURVEY	4
1.2	THE PROPOSED CONTROLLER	8
2	MATHEMATICAL FORMULATION OF THE CONTROLS	10
2.0	INTRODUCTION	10
2.1	A BRIEF INTRODUCTION TO OPTIMAL CONTROL THEORY	11
2.2	SYNTHESIS OF THE TIME OPTIMAL CONTROLLER	16
2.3	A FAST AMPLITUDE CONTROLLER	30
2.4	SYNTHESIS OF THE OPTIMAL TRACKING REGULATOR	34
2.5	A SUB-OPTIMAL TRACKING REGULATOR	40
2.6	A DUAL MODE CONTROLLER	44
3	THE CIRCUIT IMPLEMENTATION	46
3.0	INTRODUCTION	46
3.1	CIRCUIT DESIGN	47
3.1.1	The Oscillator Circuit Design	47
3.1.2	The Tracking Regulator	56
3.1.3	Dual Mode Controller Circuit Design	61
3.1.4	A Fast Amplitude Controller	64
3.2	TEST RESULTS	73
3.2.1	Distortion Measurements	73
3.2.2	Transient Response	84

CHAPTER PAGE

4 CONCLUSION 91

4.0 SUGGESTIONS FOR FURTHER RESEARCH 91

4.1 CONCLUSION 93

BIBLIOGRAPHY 95

LIST OF FIGURES

FIGURE		PAGE
1.1	A GENERALIZED AMPLITUDE CONTROL STRUCTURE	3
2.1	FAMILY OF TRAJECTORIES FOR THE HARMONIC OSCILLATOR	20
2.2	THE CONTROL U(t) AND ITS RELATIONSHIP TO $P_2(t)$	20
2.3	FAMILY OF TRAJECTORIES FOR THE HARMONIC OSCILLATOR WITH THE CONTROL APPLIED	22
2.4	THE TERMINAL CONDITIONS APPLIED TO THE OPTIMAL TRAJECTORY	22
2.5	CONSTRUCTION OF THE SWITCING CURVE	24
2.6	FURTHER CONSTRUCTION OF THE SWITCHING CURVE	24
2.7	COMPLETED CONSTRUCTION FOR THE EXTERIOR OF THE CIRCLE	25
2.8	CONSTRUCTION OF THE SWITCHING CURVE FOR THE INTERIOR OF THE CIRCLE	25
2.9	THE REGION FOR WHICH THE SWITCHING CURVE IS STILL UNDETERMINED	27
2.10	CONSTRUCTION OF THE SWITCHING CURVE FOR $\|X\| < 0.5k$	27
2.11	THE COMPLETED SWITCHING CURVE	28
2.12	THE INTERIOR SWITCHING CURVE	28
2.13	THE SIMPLIFIED SWITCHING CURVE	32
2.14	THE OPTIMAL TRAJECTORIES FOR THE TWO PERFORMANCE INDICES	39

FIGURE PAGE

2.15 THE TRANSIENT RESPONSE FOR THE OPTIMAL AND SUB-OPITMAL CONTROLS 43

2.16 THE REGION OF THE PHASE PLANE FOR WHICH STEADY STATE OPERATION IS DEFINED . . . 43

3.1 SYSTEM OVERVIEW 48

3.2 OSCILLATOR CIRCUIT DESIGN 50

3.3 OUTPUT VOLTAGES FOR A STEP-UP AND A STEP-DOWN IN AMPLITUDE 53

3.4 OP-AMP SUPPLY CURRENTS 54

3.5 OUTPUT VOLTAGE DERIVATIVES 55

3.6 TRACKING REGULATOR CIRCUIT DESIGN 57

3.7 DUAL MODE CONTROLLER CIRCUIT 62

3.8 FAST AMPLITUDE CONTROL CIRCUITRY PART 1 . . . 66

3.9 FAST AMPLITUDE CONTROL CIRCUITRY PART 2 . . . 67

3.10 FAST AMPLITUDE CONTROL CIRCUITRY PART 3 . . . 72

3.11 FREQUENCY OF OSCILLATION AND PHASE DIFFERENCE 74

3.12 DISTORTION AS A FUNCTION OF AMPLITUDE 78

3.13 THE RIPPLE VOLTAGE PRESENT IN THE CONTROL SIGNALS 79

3.14 FREQUENCY SPECTRUM FOR AN AMPLITUDE OF 10V . .80

3.15 FREQUENCY SPECTRUM FOR AN AMPLITUDE OF 10V . .81

3.16 AMPLITUDE RISE TIME 87

3.17 AMPLITUDE FALL TIME 88

3.18 PHASE PLANE PORTRAITS 89

3.19 PHASE PLANE TRANSITION 90

3.20 FAC OPERATION IN STEADY STATE 90

CHAPTER ONE: THE PROBLEM OF AMPLITUDE CONTROL

1.0 THE STRUCTURE OF AMPLITUDE CONTROL SYSTEMS

A linear oscillator would make an ideal oscillating system. However, the dependence of the amplitude on the initial conditions and designing a circuit that has poles with only imaginary components is physically impossible. Therefore, some form of nonlinearity is required. Determining that nonlinearity and the way in which it is connected in the circuit is the subject of this thesis.

There are certain criterion that must be met when designing an amplitude control system. One of the major problems is overcoming the distortion introduced by the nonlinear nature of the control. Sometimes low distortion is not the only concern; the oscillator may be required to have a fast settling time. This tends to complicate matters because a trade-off must be made between low harmonic distortion and fast settling time. For example in very low frequency oscillators a settling time of 100 to 1000 periods of oscillation is generally unacceptable. Another area of application is in automated test equipment where the oscillator acts as a signal generator; again, a fast settling time is just as important as low distortion. In an attempt to minimize both factors designers have resorted to some very novel designs with varying degrees of success. Despite the decreased settling times while distortion has remained low the trade-off still exists. The two design criterion remain linked.

Amplitude control systems have a definite structure which is illustrated in Fig. 1.1. There are three basic components to the feedback system. The first component is the magnitude detector. Its

function is to measure the amplitude of the signal. The detector is inherently a nonlinear circuit or device and consequently it is usually the largest source of distortion in the circuit. Therefore, much of the design effort centers on the detector. Following the detector is a difference amplifier which rarely poses any problems. Its main purpose is to create an error signal which is the difference between the actual and desired amplitude. The error signal then controls the variable gain amplifier which is usually the second source of distortion. As with the detector, it is inherently nonlinear; however, ideally it should be a bilinear device (ie. to have constant gain when the error signal is constant) since it would not produce any distortion. The variable gain amplifier is usually either a FET, acting as a voltage variable resistance, or an analog multiplier whose transconductance varies according to the error signal. The output of the variable gain amplifier is the control signal which feeds into the oscillator circuit and adjusts the amplitude. Figure 1.1 indicates that the input into the variable gain amplifier is V_{STATE}. V_{STATE} is a vector containing all the state variables required. In an *RC*-oscillator all state variables are voltages. Typically, only one voltage is required or controlled but this is not always so. Figure 1.1 also illustrates that the input to the magnitude detector is another vector V_{OUT} which may or may not be the same as V_{STATE}, though normally it is. Again, only a single voltage feeds into the detector in typical applications but not always. This is the basic feedback structure of an amplitude control system for which a design is sought.

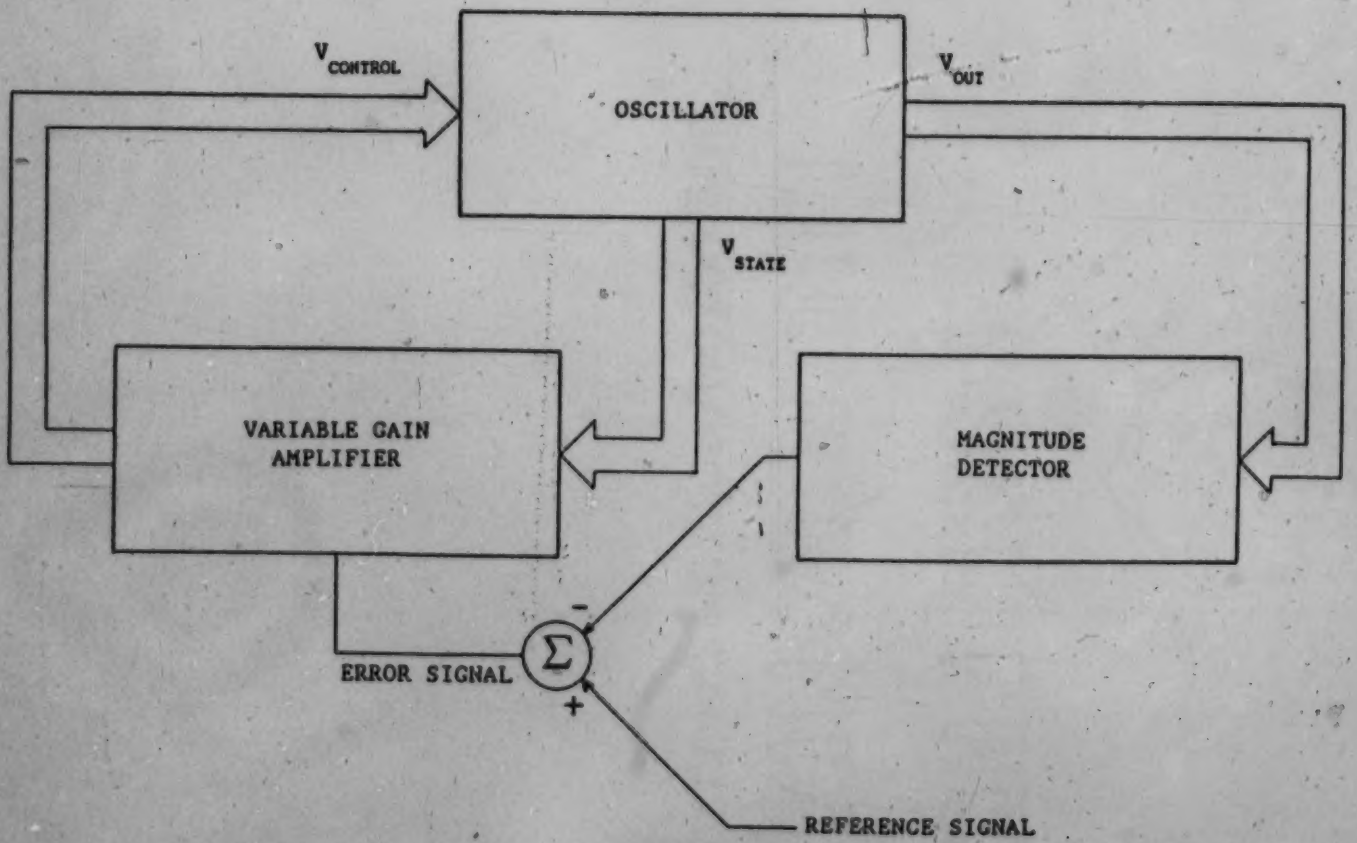

FIG. 1.1 A GENERALIZED AMPLITUDE CONTROL STRUCTURE

1.1 LITERATURE SURVEY

The typical approach (see [1] and [2]) to designing an amplitude control system is to use a rectifier as the detector. This is followed by a filter creating a smooth dc signal which can then be compared with the reference signal. The larger the time constant of the filter the less harmonics there will be. At the same time the transient duration will increase. In order to obtain a total harmonic distortion (THD) of 0.1% the time constant of the filter needs to be large enough that a settling time of several hundred periods of oscillation will result [5]. This is why so much effort has been placed in creating new designs for the magnitude detector.

Efforts of various designers to overcome the problem have resulted in methods which can be categorized into four groups. The first group ([3]-[6]), replaces the rectifier and filter with a sample and hold peak detector synchronised to the oscillation frequency. The circuit by Vannerson [5] will serve as an example. the approach is applied to a quadrature phase or state variable oscillator which has two outputs whose phase difference is 90°. Vannerson exploits the fact that when the first output is zero the second output has reached its peak. By sensing the zero crossing of the first output with an edge sensitive comparator the resulting output can be used to control the sample and hold so that it samples the peak value of the second output. Once the peak value has been obtained the circuit follows the same pattern as described in section 1.0, where in this example the variable gain amplifier is realized with an analog multiplier. The THD is better than 0.001% and the settling time is two or three periods of oscillation. The frequency of oscillation is limited by

the bandwidth of the sample and hold, and low distortion figures are obtained only if the sampling time is less than 0.05 times the period of oscillation.

It has been stated that a linear oscillator could not be built because the initial conditions could not be predetermined. What if they could? The second design approach ([7]-[9]) attempts to do just that. In an *RC*-oscillator all state variables are voltages determined by the capacitors; therefore, it is the charge on the capacitor which determines the initial condition. In this approach the control circuit waits until the energy in the capacitor is zero and then places a charge on the capacitor equivalent to the desired amplitude once each period. In the paper by Filanovsky [9], the settling time was one period of oscillation while maintaining a THD of less than 0.2% for a range of amplitudes from 2 to 7V.

The above two methods relied on sampling of the oscillator's signals to determine the control. The third group ([10],[11]) departs from this approach. Instead the attempt is done to eliminate the filter or at least significantly reduce the time constant. The approach is to use a multi-phase rectifier. The circuit by Vannerson [11] uses the quadrature phase oscillator as before but takes the two outputs; inverts them; to create four outputs that are all 90° out of phase. These outputs are then rectified and summed. The result is an output voltage with very little ripple and a filter with a small time constant can remove that. For a THD of 0.004% the settling time is 250 periods. However, the THD can be traded-off for speed. For example, the settling time can be redueced to 1.5 periods if a THD of 0.6% is acceptable.

The final method ([12],[17]) is similar to the third in that it eliminates the filter. However, the means of measuring the amplitude involves analog computation. The idea is to exploit the phase relationship of the quadrature phase oscillator. If the two outputs are squared and then summed, the result is a dc signal which is equivalent to the amplitude. There are, however, several weaknesses to this approach. The first is that the squaring circuits should be matched. If not distortion will occur. The phase error of the two voltages must be small. However, the results can be quite good; in [2] a THD of 0.005% to 0.06% depending on amplitude was achieved. Typical settling times are between 6 to 10 periods.

The quadrature phase oscillator is not the only circuit for which this control can be applied. It can also be used in the twin-T oscillator since the phase difference of the voltages at the nodes of each T network is 90°. The method can also be extended [6] to other multiphase oscillators. For example, if an oscillator has three outputs each 120° apart, then if these voltages are squared and summed, the result is a dc voltage 1.5 times the amplitude.

THD figures and settling times have been used as a basis for comparison, an important factor has been ignored in these comparisons, namely, frequency. Frequency also has an effect on the distortion and settling times obtained. The problem is that not every researcher records what the frequency of his circuit was, which creates some doubts as to the validity of the comparison. To make matters worse, some researchers do not record the conditions under which the measurements were made. For example, a low distortion figure is obtained as well as fast settling time but were they obtained at the

same time with the same circuit conditions? Therefore, it is not as easy as it appears to judge the merits of the designs based on just the published results.

From this survey it is clear that various designs have obtained improved results as compared to the typical design. Each has its advantages and disadvantages. There is one thing that remains common to all of them; low distortion and fast settling remain contradictory design criterion requiring the designer to make a trade-off.

1.2 THE PROPOSED CONTROLLER

The first step in designing the amplitude controller is to sever the link between response time and distortion. The only time to be concerned about settling time is during amplitude transitions whereas one only needs to be concerned about distortion during steady state behavior. Since transient and steady state behavior represent two separate parts of the dynamic behavior why not have two separate controls: one for steady state behavior whose only design criterion is low distortion and one for transient behavior which is optimized for fast response. This way no trade-off has to be made.

First, consider the control that has a fast response. Of all the designs discussed in section 1.1 none of them were copied or modified here. Instead the results of optimal control theory were applied to synthesize a control. Many of the papers discussed claimed that their control was fast. The intent here was to design a controller that was the fastest. Optimal control theory was used to determine the control law that minimized the time of transition from one amplitude to the other. The nature of the control is unlike any other but the design of the fast amplitude control was only half the problem.

Having used optimal control for one controller it was only natural to try it for the steady state controller. However, it is not possible to state a performance index that minimizes the distortion directly. This is because the mathematical model or description has no harmonics as long as a system is chosen such that the limit cycle is circular. The harmonics are due to the non-idealities of the circuit; deviations from the model caused by the circuit. Since the model is synthesized before the circuit is designed the anomalies

cannot be accounted for. Instead the error between the actual and the desired amplitude is minimized over an infinite amount of time. This at least ensures that the limit cycle is circular.

The thesis is divided into four chapters including this one. Chapter two delves into the world of mathematics and optimal control. The optimal solutions are found but due to their complexity sub-optimal controls are derived. These proposed controls provide the basis of the circuit design which is covered in chapter three. The final chapter is the conclusion and brings this treatise to a close.

CHAPTER TWO: MATHEMATICAL FORMULATION OF THE CONTROLS

2.0 INTRODUCTION

This chapter discusses the mathematics used to design the control systems. The notation and nomenclature of optimal control theory is first introduced and then a basic summary of the results is covered. The coverage is brief and the reader is referred to the references cited in the text for more in-depth information. This is followed by a discussion of time optimal control. The results here are applied to solving the time optimal control for an oscillator where the goal is to reach a desired amplitude in the shortest time. Discussion continues with the proposed controller which is the control system that was actually built. It is a sub-optimal control based on the solution of the optimal control. The discussion then turns to the optimal tracking regulator. This control system takes over after the desired amplitude in the oscillator is reached. Its main job is to ensure that the oscillator stays at the desired amplitude and hopefully does not introduce too much distortion in the process. The results of the optimal tracking regulator are found to have some drawbacks and so a sub-optimal controller is proposed that is more feasible in terms of the circuit design. It is also found that this control has a faster rate of convergence than the optimal control and reasons for this are discussed. Finally, the chapter concludes by looking at a dual mode control system. The dual mode control simply determines when the two different control systems should be applied to the oscillator.

2.1 A BRIEF INTRODUCTION TO OPTIMAL CONTROL THEORY

Once a mathematical model of the oscillator has been attained the design of the control system can begin. The results of optimal control theory can be used to determine the nature of the control. However, in order to use these results, one must be familiar with the concepts, language and notation of the theory. This section introduces the notation used in this thesis when discussing optimal control and includes the following topics:

- state space modelling of the oscillator,
- introduction of the performance index J,
- discussion of the terminal conditions,
- incorporation of the constraints into J,
- introduction of the Hamiltonian H,
- statement of the necessary conditions for optimization,
- statement of the associated terminal conditions.

In order to apply optimal control theory the design must have precisely defined goals and the system must be modelled mathematically. The results of optimal control theory are usually stated using a state space representation; therefore, the equations governing the oscillator must be written in that form. The general form of the equation is

$$\dot{\mathbf{x}} = \mathbf{f}(\mathbf{x},\mathbf{u},t) \qquad t \in [t_o, t_f] \tag{2.1}$$

where $\mathbf{x}$ is an n vector controlled by $\mathbf{u}$, an m vector, and the initial condition

$$\mathbf{x}(t_o) = \mathbf{x}_o. \tag{2.2}$$

Since only linear time invariant equations are studied, equation (2.1) can be re-written as

$$\dot{x} = Ax(t) + Bu(t) \qquad (2.3)$$

where the oscillatory nature of the system is determined by the eigenvalues of A.

With a state space model of the system, the design goals are then expressed in terms of a performance index J[1] where

$$J = \psi[x(t_f)] + \int_{t_o}^{t_f} \phi[x(t),u(t)]dt \qquad (2.4).$$

The problem is incomplete unless a set of relations is imposed on the terminal point of the trajectory. This is usually stated by a q-dimensional terminal manifold given by

$$N[x(t_f),t_f] = 0 \qquad (2.5).$$

The objective is to minimize J with respect to the control $u(t)$ subject to the equality constraints: the differential equation (2.3), the initial condition (2.2) and the terminal condition (2.5). Lagrange multipliers are used to incorporate these constraints into the formulation for J. Introducing $p(t)$, an n dimensional costate vector for $x(t)$, and ℓ, a q dimensional Lagrange multiplier for N, the equality constraints are adjoined to J as follows:

$$J = \psi[x(t_f)] + \ell^T N[x(t_f),t_f] + \int_{t_o}^{t_f} \Big\{ \phi[x(t),u(t)] + p^T(t)[Ax(t) + Bu(t) - \dot{x}] \Big\} dt \qquad (2.6).$$

To make the notation more compact H, the Hamiltonian, is introduced. H is defined as

---

1 J is sometimes referred to as a cost functional

$$H[x(t),u(t),p(t)] = \phi[x(t),u(t)] + p^T(t)[Ax(t)+Bu(t)] \quad (2.7),$$

then J becomes

$$J = \psi[x(t_f)] + \nu^T N[x(t_f),t_f] + \int_{t_o}^{t_f}\left\{H[x(t),u(t),p(t)] - p^T\dot{x}\right\} dt \quad (2.8).$$

In equation (2.8) t_f may be unknown, therefore the condition for a minimum will be altered to reflect that fact or t_f can be allowed to approach infinity producing an improper integral. Furthermore, inequality constraints can be imposed on $u(t)$. In order to solve the problem with inequality control constraints Pontryagin's Principle [12] is used . Other conditions such as state inequality constraints could be imposed, but they are not discussed in this thesis. With the design goals now incorporated into J and the constraints imposed by the system and endpoint conditions, J is ready to be minimized.

J is minimized by computing the first variation δJ and setting $\delta J = 0$. From this the necessary conditions for $u(t)$ to minimize J are

$$\frac{\partial H}{\partial p} = \dot{x} = Ax(t) + Bu(t) \quad (2.9)$$

$$\frac{\partial H}{\partial x} = -\dot{p} = \frac{\partial \phi}{\partial x} + A^T p(t) \quad (2.10).$$

If there are no constraints imposed on $u(t)$ then the relation

$$\frac{\partial H}{\partial u} = 0 = \frac{\partial \phi}{\partial u} + B^T p(t) \quad (2.11)$$

is used. However, if $u(t)$ is bounded such that $u(t) \in \Omega$ where Ω is the set of admissible values of controls then

$$H[x(t),\hat{u}(t),p(t)] \leq H[x(t),u(t),p(t)] \quad (2.12)$$

where $\hat{u}(t)$ is the optimal control. Equation (2.9) is the original

system of n first order differential equations. Added to (2.9) is (2.10) with another n equations to solve. Associated with these equations are $2n$ arbitrary constants. The information required to determine these constants comes from the endpoint conditions which are:

$$x(t_o) = x_o \tag{2.13}$$

$$N\,[x(t_f)] = 0 \tag{2.14}$$

$$\frac{\partial \theta}{\partial x(t_f)} + \left[\frac{\partial N^T}{\partial x(t_f)}\right] \ell \cdot p(t_f) = 0 \tag{2.15}$$

and if t_f is unspecified the relation

$$\frac{\partial \theta}{\partial t_f} + \left[\frac{\partial N^T}{\partial t_f}\right] \ell \cdot H = 0 \tag{2.16}$$

is added. Equations (2.9) to (2.16) comprise the necessary conditions for the minimization of J and (2.13) to (2.16) the endpoint conditions.

If it is possible for J to be maximized, an investigation of the second variation $\delta^2 J$ is required to determine whether J has been maximized or minimized. However, in the problems studied, it is usually apparent from the solution which extreme has been reached and the computation of $\delta^2 J$ is not required.

Although optimal control theory provides a mathematically optimal solution, a problem arises when the solution is viewed from an engineering standpoint. First and foremost $u(t)$ should be a function of $x(t)$, the state, in order that a feedback control law is obtained. Because the system of equations is almost always a two-point boundary value problem, the solution obtained is in the form of an open loop

control. Formulating the problem in terms of the Hamilton-Jacobi [13] equation will provide a feedback control law when solved. However, the Hamilton-Jacobi equation is a partial differential equation and is not easily solved. The only other approach is to make the assumption that u is a function of x, i.e. u[x(t)], then apply the assumption to the equations and hope it works. This approach is implicit in the solutions that follow.

Although the performance index J has been introduced as a means for expressing the design goals in mathematical terms, J does not describe the entire problem. Endpoint conditions are required to supplement the information already obtained about the problem. Depending on whether any bounds on u are imposed, either equation (2.11) or (2.12) is used. If (2.12) is used, the optimal trajectory x will normally have "corners". An example of this occurs in the next section on time optimal control. This section has introduced optimal control theory but not in any general terms. More general and more thorough treatments can be found in Sage [13] and Athans and Falb [14]. A concise but complete statement of the theory can be found in Macki [16].

2.2 SYNTHESIS OF THE TIME OPTIMAL CONTROLLER

This section now applies the results of the previous section to the problem of time optimal control. This particular problem of the time optimal control applied to the harmonic oscillator is one that appears extensively in the literature as it provides a simple example. However, for the majority of the research literature examined the target set or terminal set has always been the origin. What this means is that the optimal control has been used to damp out the oscillations. This is not the case here; on the contrary, the aim here is to have the system achieve a desired amplitude in the shortest possible time. This section will outline the solution to this problem. Much of the work depends on the geometrical description of the state variable trajectories in the phase plane. The following topics are covered:

- the constraints on u,
- the performance index J for this problem,
- the optimal control $\hat{u}$ in terms of $p(t)$,
- a graphical solution based on the information from the terminal manifold and its gradient,
- a switching curve for $u(t)$ from the graphical solution,
- a feedback control law.

The time optimal problem can be made more precise by putting it in mathematical terms. Equation (2.3) is repeated here for reference and it describes the linear harmonic oscillator for which an amplitude controller is desired;

$$\dot{x} = Ax(t) + Bu(t) \qquad (2.17)$$

where A is given as

$$A = \begin{bmatrix} 0 & \beta \\ -\beta & 0 \end{bmatrix} \tag{2.18}$$

and β determines the frequency of oscillation. If $u(t) = 0$ then

$$\begin{bmatrix} x_1(t) \\ x_2(t) \end{bmatrix} = \begin{bmatrix} \sqrt{x_{10}^2 + x_{20}^2}\ \sin(\beta t+\xi) \\ \sqrt{x_{10}^2 + x_{20}^2}\ \cos(\beta t+\xi) \end{bmatrix} \tag{2.19}$$

In the x_1x_2 plane the solution is a family of circles centered at the origin (see Fig. 2.1) where the amplitude is determined by the initial conditions. To keep the controller simple only a single control will be designed, that is, $m = 1$. The circuit realization of the control will have limits on the voltages it can produce. It is, therefore, expected that $u(t)$ will have upper and lower bounds. Assuming that the voltage swing is symmetrical the inequality is given as

$$|u(t)| < k \tag{2.20}$$

where k is a positive constant. However, it is more convenient to write (2.20) as

$$|u(t)| < 1 \tag{2.21}$$

where the constant k is incorporated into the matrix B. Since B is a 2 x 1 matrix it will be represented as a vector b.

Since the only objective is to minimize the time

$$\psi = t_o = 0, \quad \phi = 1 \tag{2.22}$$

therefore, J is

$$J = \int_0^{t_f} dt = t_f \tag{2.23}$$

The results of the previous section can now be applied. The Hamiltonian is

$$H[x,u,p] = 1 + p^T[Ax + Bu]$$

$$= p^TAx + p^Tbu \qquad (2.24).$$

Applying the inequality (2.12)

$$H[x,\hat{u},p] \leq H[x,u,p] \quad |u(t)| \leq 1 \qquad (2.25)$$

$$1 + p^T(t)Ax(t) + p^Tb\hat{u}(t) \leq 1 + p^T(t)Ax(t) + p^Tbu(t) \qquad (2.26)$$

$$p^T(t)b\hat{u}(t) \leq p^T(t)bu(t) \qquad (2.27).$$

Letting $p^T(t)b = q(t)$, a scalar, there is a $\hat{u}(t)$ which minimizes the function

$$\varphi = q(t)u(t) \qquad (2.28).$$

It is apparent that

$$\min \varphi = \min (q(t)u(t)) = -|q(t)| \qquad (2.29)$$

therefore $\hat{u}(t)$ must be

$$\hat{u}(t) = +1 \quad \text{if } q(t) < 0$$

$$\hat{u}(t) = -1 \quad \text{if } q(t) > 0 \qquad (2.30).$$

$\hat{u}(t)$ is indeterminate if $q(t) = 0$

In more compact notation

$$\hat{u}(t) = -\text{sgn}(q(t)) = -\text{sgn}(p^T(t)b) \qquad (2.31).$$

Now the results of equations (2.9) and (2.10) can be applied.

$$\frac{\partial H}{\partial p} = \dot{x} = Ax(t) + bu(t) = Ax(t) - b\ \text{sgn}[p^T(t)b] \qquad (2.32)$$

$$\frac{\partial H}{\partial x} = -\dot{p} = A^Tp(t) \qquad (2.33)$$

A is skew symmetric, thus (2.33) becomes

$$\dot{p} = Ap(t) \qquad (2.34)$$

The solution to (2.34) is

$$p(t) = e^{At}p(0) \qquad (2.35)$$

where

$$e^{At} = \begin{bmatrix} \cos \beta t & \sin \beta t \\ \sin \beta t & \cos \beta t \end{bmatrix} \qquad (2.36).$$

In equation (2.30) if $q(t) = 0$ then $\hat{u}(t)$ is undetermined. If $q(t) = 0$ over an interval of time, say $[t_1, t_2]$, then the control problem is a singular control problem. Otherwise, it is called a normal control problem [14]. Since $q(t) = p^T(t)b$, the only way $q(t)$ could be zero over an interval of time is if $p^T(t)b$ is zero over an interval. From Equation (2.35) and (2.36) it is clearly seen that this is impossible; therefore, the control problem is normal and there is no need for concern over a singular solution.

The endpoint conditions can now be applied to the problem. The terminal manifold or the target set is

$$N[x(t_f)] = x_1^2(t_f) + x_2^2(t_f) - R_o^2 = 0 \qquad (2.37)$$

where R_o is the desired amplitude. Equation (2.37) describes a circle in the x_1x_2 plane with radius R_o and the center at the origin. Applying (2.16)

$$H[x(t_f), p(t_f)] = 0 = p^T(t_f)Ax(t_f) - p^T(t_f)b \operatorname{sgn}[p^T(t_f)b] \qquad (2.38).$$

Since $\frac{\partial H}{\partial t} = 0$ this result can be extended to cover the entire interval, thus

$$H[x(t), p(t)] = 0 \qquad \forall t \in [0, t_f] \qquad (2.39)$$

and from equation (2.15)

$$p(t_f) = \ell \begin{bmatrix} 2x_1(t_f) \\ 2x_2(t_f) \end{bmatrix} \qquad (2.40).$$

One additional fact is that $p(t_f)$ is normal to the target set [14], which is implied in (2.40) since $\frac{\partial N}{\partial x}$ is the gradient of N. Now let

$$b = \begin{bmatrix} 0 \\ k \end{bmatrix} \qquad (2.41)$$

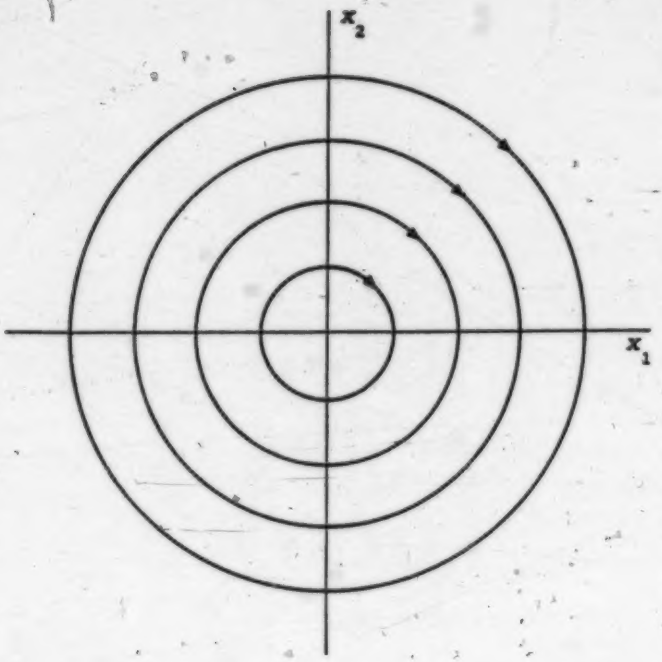

FIG. 2.1 FAMILY OF TRAJECTORIES FOR THE HARMONIC OSCILLATOR

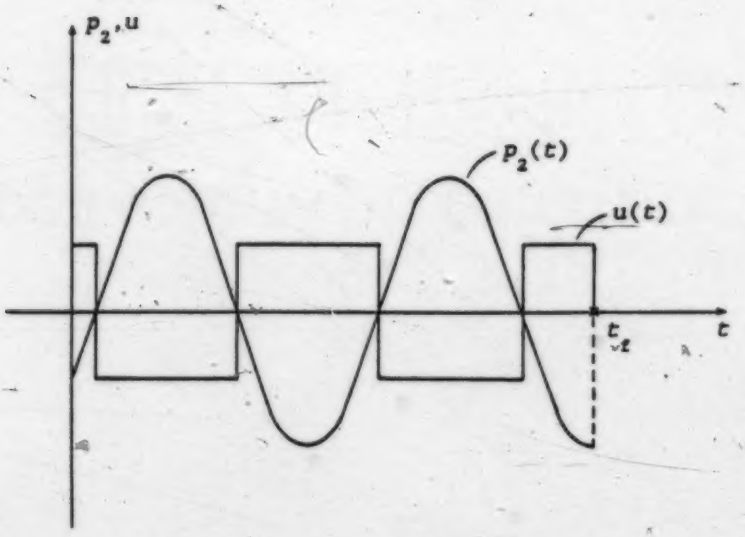

FIG. 2.2 THE CONTROL U(T) AND ITS RELATIONSHIP TO P2(T)

thus the control will only be applied to x_2 and

$$q(t) = p_2(t)k \tag{2.42}$$

In Fig. 2.2 $p_2(t)$ is plotted and $u(t)$ has been superimposed. From the graph it is apparent that $u(t)$ is a piecewise constant function, it can remain constant for no more than $\frac{\pi}{\beta}$ units of time, and there is no upper bound on the number of switchings. Essentially, $u(t)$ is a square wave with frequency β until such time as the target set is reached.

Letting

$$u = \Delta = \pm 1 \tag{2.43}$$

the system (2.17) is solved for $u(t)$ - a constant. The solution of the system is

$$x_1(t) = \left(x_{10} - \frac{k\Delta}{\beta}\right)\cos \beta t + x_{20}\sin \beta t + \frac{k\Delta}{\beta}$$

$$x_2(t) = -\left(x_{10} - \frac{k\Delta}{\beta}\right)\sin \beta t + x_{20}\cos \beta t \tag{2.44}.$$

The time dependence can be eliminated from (2.44) which gives

$$(\beta x_1 - k\Delta)^2+(\beta x_2)^2 = (\beta x_{10} - k\Delta)^2+(\beta x_{20})^2$$

$$= \text{constant} \tag{2.45}.$$

Equation (2.45) is drawn in Fig 2.3. As illustrated, the trajectories are circles with centers $(-k,0)$ and $(k,0)$ in the $\beta x_1 \beta x_2$ plane.

With the information obtained the switching curve for $u(t)$ in the $\beta x_1 \beta x_2$ plane can now be determined. To begin, assume R_o in (2.37) is

$$R_o = 2.5k \tag{2.49}$$

and that the initial point $\mathbf{x}_o$ lies outside the circle described by $N[\mathbf{x}(t_f)]$. Let $\mathbf{x}_f$, the final point, be expressed parametrically as

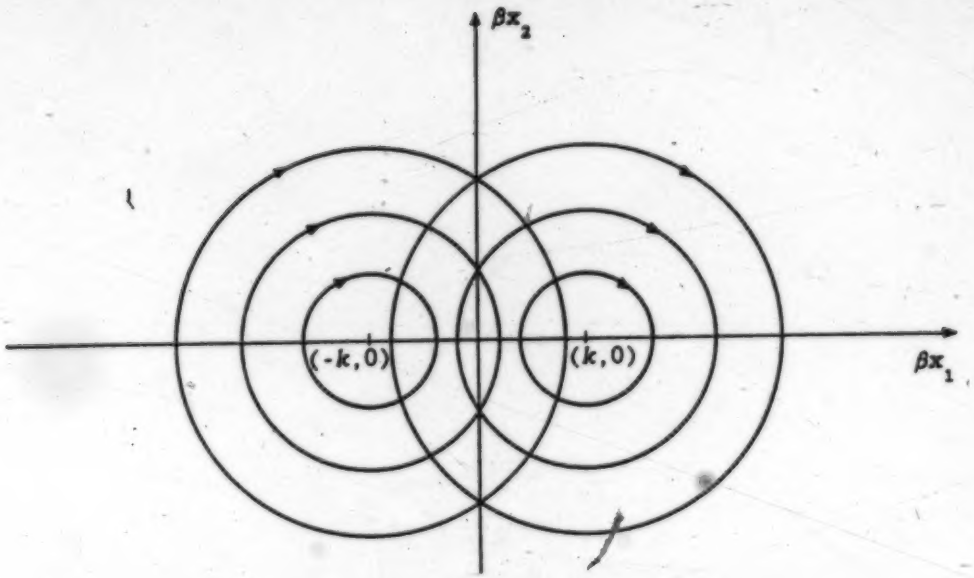

FIG. 2.3 FAMILY OF TRAJECTORIES FOR THE HARMONIC OSCILLATOR WITH THE CONTROL APPLIED

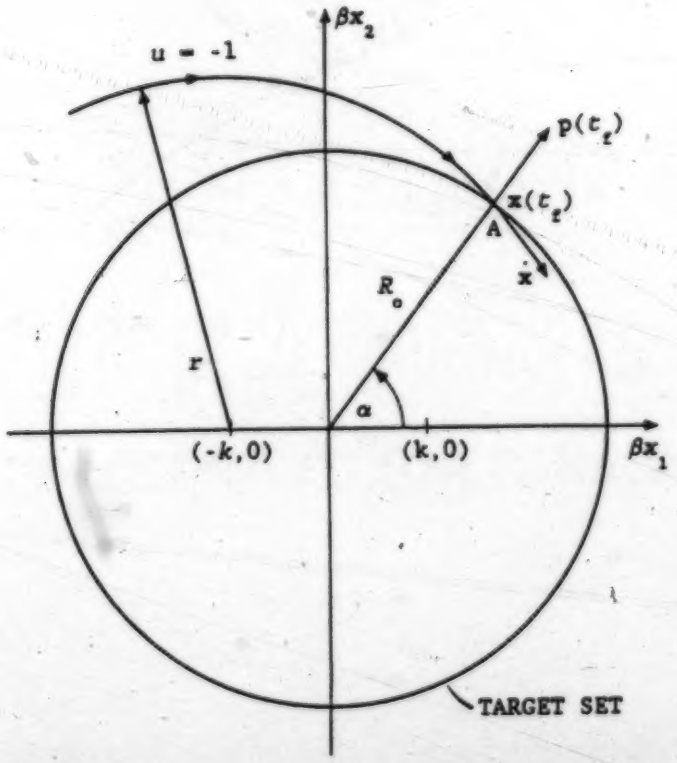

FIG. 2.4 THE TERMINAL CONDITIONS APPLIED TO THE OPTIMAL TRAJECTORY

$$x_f = \begin{bmatrix} R_o \cos \alpha \\ R_o \sin \alpha \end{bmatrix} \qquad (2.50).$$

From the previous discussion it is known that $p(t_f)$ is normal to the target set (Fig 2.4). Since it is the direction rather than the magnitude of $p(t_f)$ that is of concern, let

$$p(t_f) = \begin{bmatrix} \cos \alpha \\ \sin \alpha \end{bmatrix} \qquad (2.51).$$

Using (2.51) as the terminal condition for (2.35) the arbitrary constants can be solved for in terms of α and t_f giving,

$$p(t) = \begin{bmatrix} \cos (\beta t_f + \alpha - \beta t) \\ \sin (\beta t_f + \alpha - \beta t) \end{bmatrix} \qquad (2.52).$$

In Fig. 2.4 it can be seen that for $0 < \alpha < \pi$ $u(t) = -1$. Because

$$u(t) = -\text{sgn}[p_2(t)k] \qquad (2.53)$$

$p_2(t)$ must be positive. In order that $p_2(t) > 0$ the following must be true,

$$\beta t_f - (\pi - \alpha) < \beta t < \beta t_f + \alpha \qquad (2.54).$$

However, βt will never exceed βt_f and (2.54) can be modified to

$$\beta t_f - (\pi - \alpha) < \beta t < \beta t_f \qquad (2.55).$$

Starting at the point A and tracing the trajectory backwards in time until the control switches, the angle of the arc traced will be $\pi - \alpha$ radians, as determined from (2.55). If the point where $u(t)$ switches is called B then as α varies from 0 to π the point B will trace a semicircle with radius k and center $(-(R_o + k), 0)$ (see Fig. 2.5). The semicircle is part of the switching curve. The switchings of $u(t)$ will now occur every π radians until x_o is reached (Fig. 2.6). Thus, outside of the target set the $\beta x_1 \beta x_2$ plane is divided in half by a series of connecting semicircles (Fig. 2.7) with radius k. In the

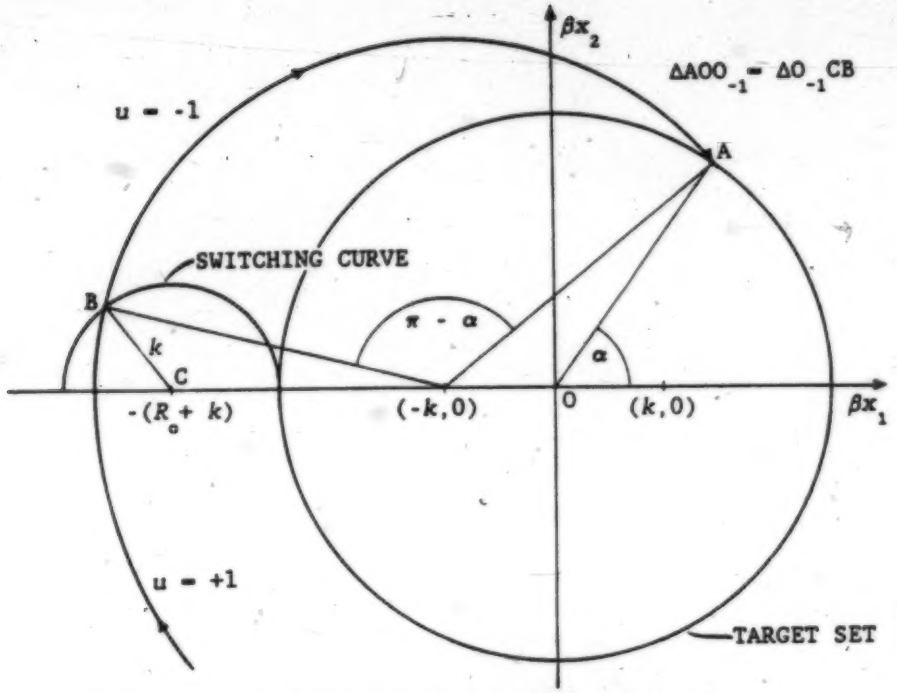

FIG. 2.5 CONSTRUCTION OF THE SWITCHING CURVE

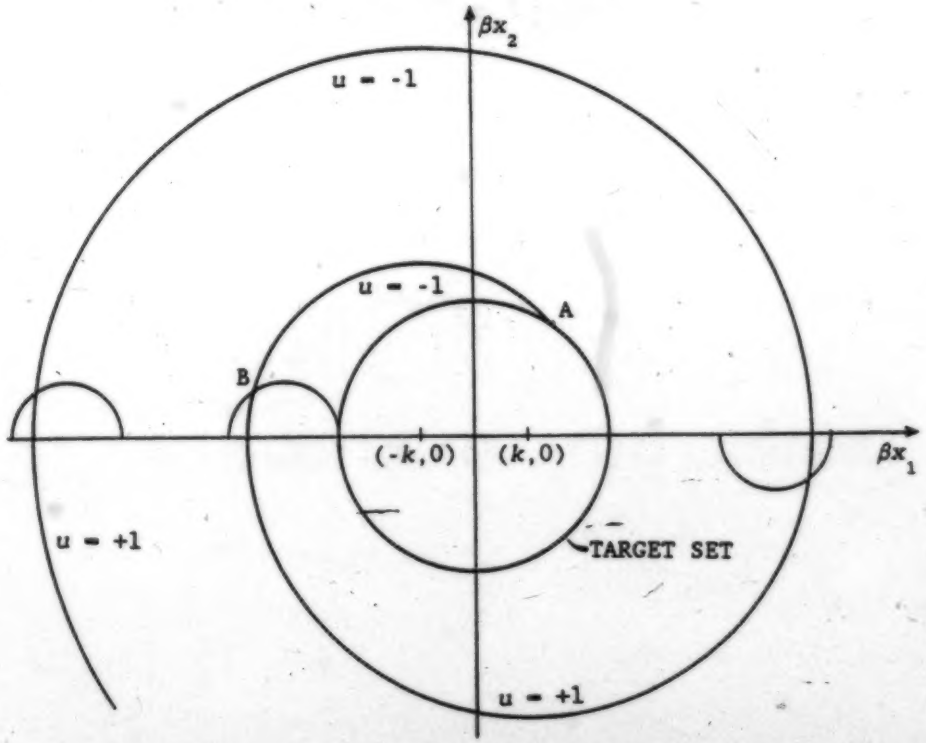

FIG. 2.6 FURTHER CONSTRUCTION OF THE SWITCHING CURVE

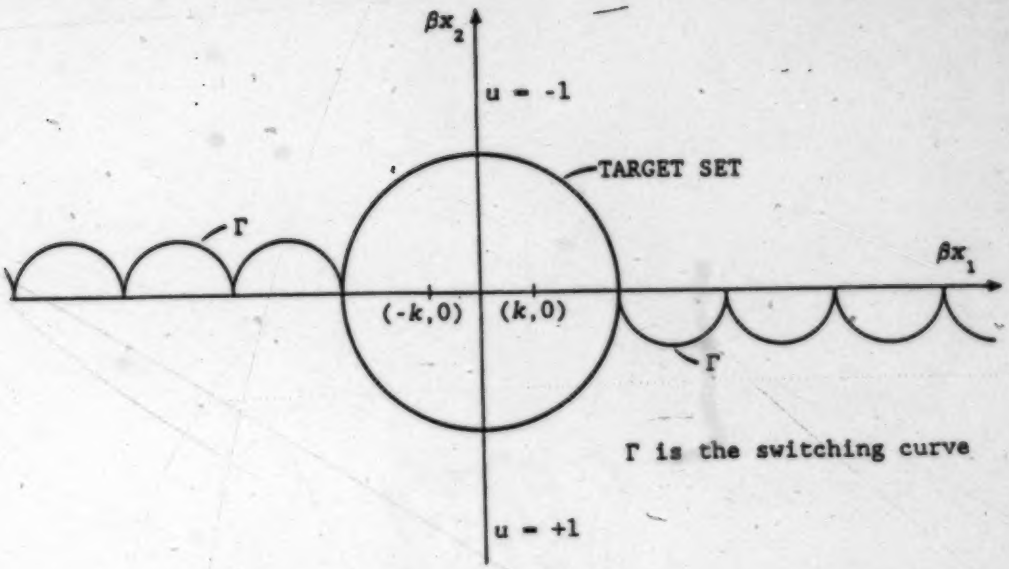

FIG. 2.7 COMPLETED CONSTRUCTION FOR THE EXTERIOR OF THE CIRCLE

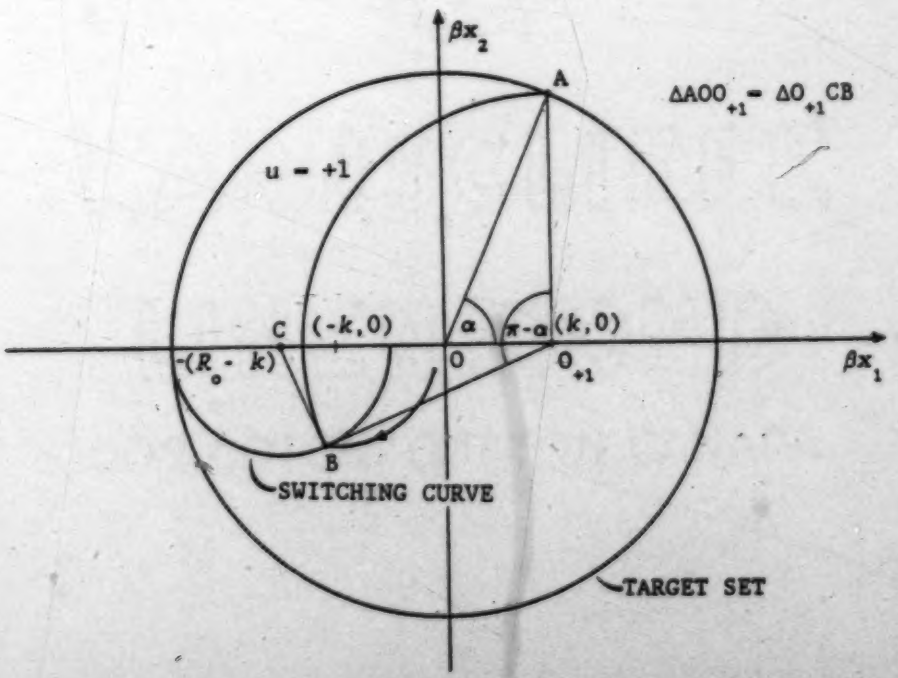

FIG. 2.8 CONSTRUCTION OF THE SWITCHING CURVE FOR THE INTERIOR OF THE CIRCLE

upper half plane $u = -1$ and in the lower half plane $u = +1$. When the trajectory reaches one of the semicircles the control switches, hence the name switching curve.

Having determined the switching curve outside the circle, the switching curve inside the circle will now be determined. The argument here is completely analogous to that already presented except that for $0 < \alpha < \pi$ the control $u(t) = +1$ and the vector $p(t_f)$ points into the circle. However, the conclusion that the angle of the arc is $\pi-\alpha$ radians still remains true (see Fig. 2.8). As before, as α varies from 0 to π B traces a semicircle. The semicircle represents part of the switching curve for the interior of the circle. However, the next part of the switching curve is not determined by tracing several trajectories of angle π radians from the semicircle described by B. In fact, the situation becomes complicated and requires some explanation. In Fig. 2.9 the circular target set is drawn. In its interior have been drawn the two semicircular switching curves; one for $u = +1$ and the other for $u = -1$. The only part of the $\beta x_1 \beta x_2$ plane for which the switching curves is not known is for

$$\sqrt{x_1^2 + x_2^2} < 0.5k \qquad (2.56).$$

To aid the discussion below, let the semicircle on the left be L and the one on the right R. The switching curve for the condition specified in (2.56) is determined by the locus for which the transition time to the target set is equal regardless of whether the starting value for the control is $u(t)=+1$ or $u(t)=-1$. This is the same as determining the point for which the sum of the angles θ_1 and θ_4 is equal to the sum of the angles θ_2 and θ_3 as depicted in Fig. 2.10. The problem is best solved numerically and the solution is

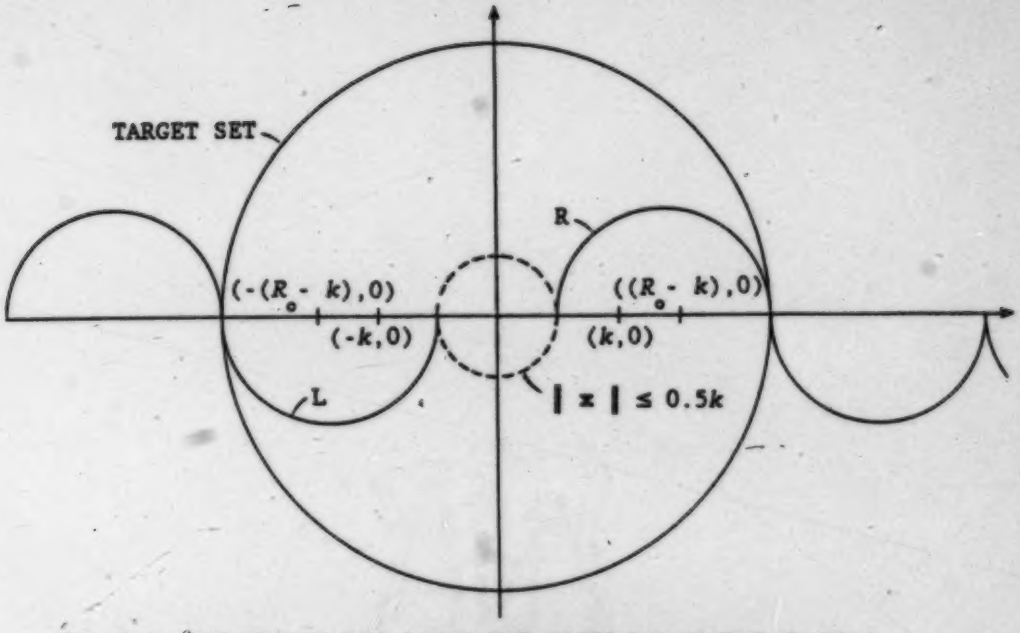

FIG. 2.9 THE REGION FOR WHICH THE SWITCHING CURVE IS STILL UNDETERMINED

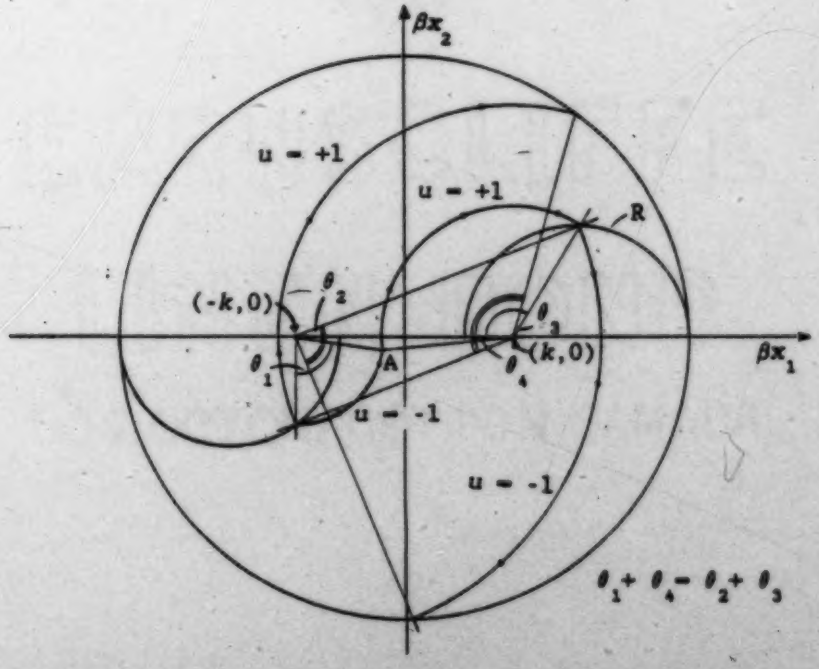

FIG. 2.10 CONSTRUCTION OF THE SWITCHING CURVE FOR ||x|| < 0.5k

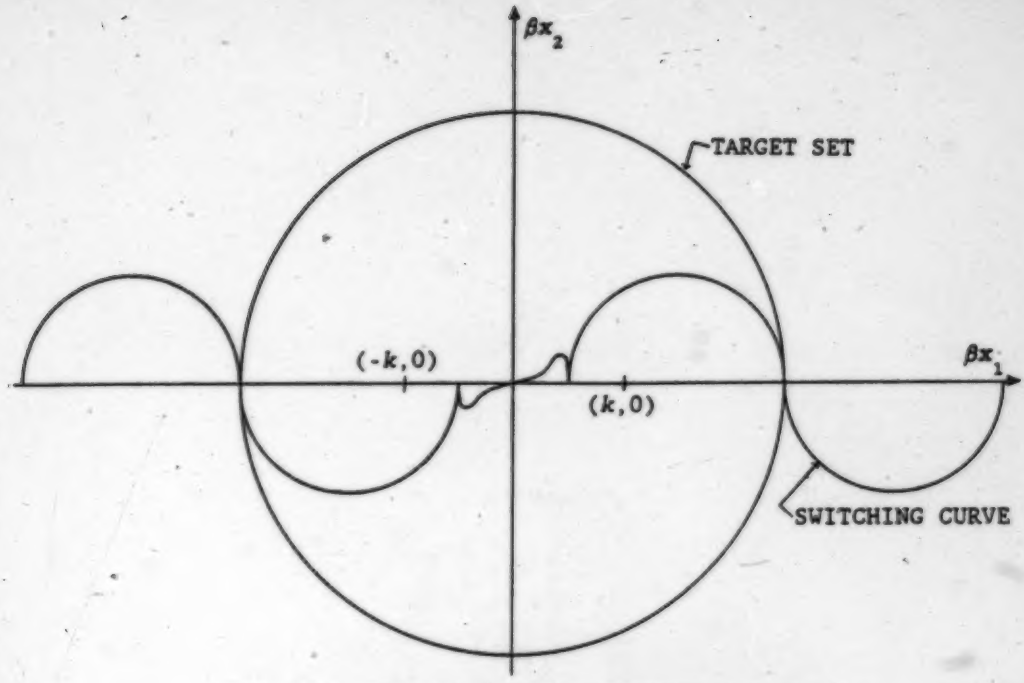

FIG. 2.11 THE COMPLETED SWITCHING CURVE

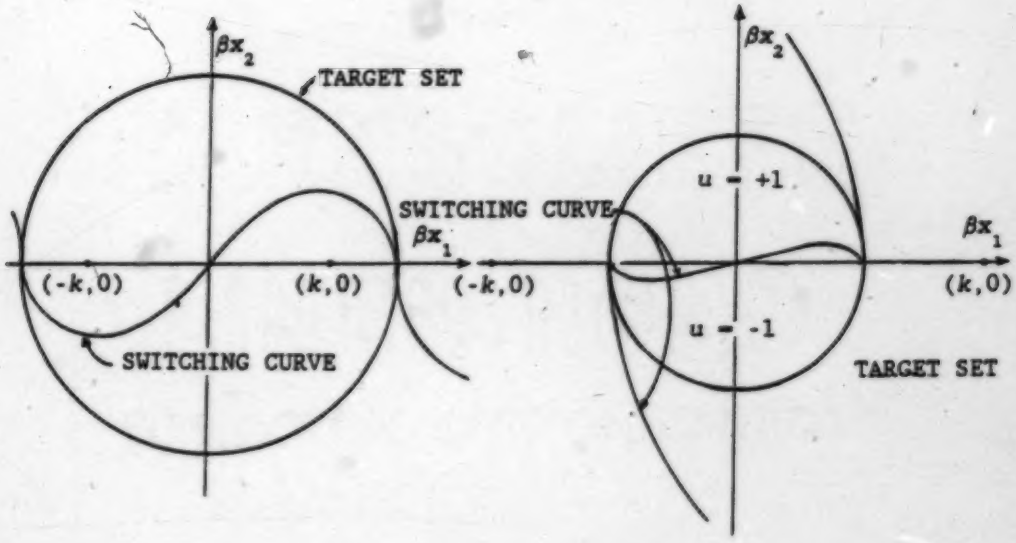

a) $R_o = 1.5k$ b) $R_o = 0.5k$

FIG. 2.12 THE INTERIOR SWITCHING CURVE

shown in Fig 2.11. In the design of the oscillator R_o will change. Because R_o does change, the switching curve in the region defined by (2.56) changes too, as illustrated in Figs. 2.10 to 2.11. Therefore, even if a switching curve were realizable for a specific R_o the fact that the curve changes as R_o changes makes an engineering solution unviable.

If $R_o < 2k$ then the switching curve in the interior of the circle will be determined solely by the equal angles argument since no switching of the control occurs. In Fig 2.12a and b the switching curves are shown for $R_o = 1.5k$ and $R_o = 0.5k$ respectively. Since these curves are determined numerically this precludes any sort of engineering realization. The curve is too complex and an approximation must be sought. Thus, the only possible design that can emerge from this theoretical discussion is a sub-optimal one. However, a standard of comparison has been obtained and thus sub-optimal designs can be judged on how well they approach the optimal solution.

This section has determined the time optimal control for a harmonic oscillator with a circular target set. Determining the switching curve resulted in the solution being stated as a feedback control law. Although the solution is not realizable it does give a standard to aim for. It should be pointed out that the graphical approach used provided considerable insight into the solution of the problem.

2.3 A FAST AMPLITUDE CONTROLLER

The time optimal control law as stated in the previous section could only be synthesized in terms of a circuit with great complexity. The most obvious approach would be a digital one. However, that is not one of the options open. The circuit is essentially an analog one and it does its processing continuously. It is also an advantage if the circuit can be simplified at the cost of a little performance. The major problem with the time optimal controller is the switching curve; it is too complex. In this section a slightly modified control law will be introduced with a simpler and restricted switching curve.

The consideration is to determine the region of the phase plane that is of importance. It is obvious that there is a limit to the magnitude of the voltages or currents that can be obtained with the circuit chosen which, therefore, limits or restricts the region of the phase plane that is applicable to the control. The parameter that will determine the restriction is k, but k was not known previously. In order to get some idea of what k is an initial design was made. It was decided that the maximum voltage that could be allowed in the circuit was ±10 volts. It was the voltage restriction rather than k that became the final design parameter. If the maximum allowed voltage is V_{MAX} then

$$V_{MAX} = \frac{k}{\beta} \tag{2.57}$$

In the βx_1-βx_2 plane this means that the centers for the circular trajectories would always be outside the target set. Therefore, only a portion of the semi-circle needs to be simulated in both the right and the left sides of the plane. This applies to points outside the target set. For points inside the circle, the switching curve can be

simplified by letting it be the x_1 axis. Since the centers for the arcs that would result are outside the target set, the radii of those arcs will be relatively large and therefore, the error introduced by the approximation should be small. Fig. 2.13 shows the division of the plane and the proposed switching curve.

The control has been obtained for the oscillator but only in terms of a switching curve which has been represented graphically. In order to design the circuitry the control law must be expressed explicitly in mathematical terms. The first step in doing that is to divide the applicable area depicted in Fig. 2.13 into regions. First, create two regions: one for where the control $u(t)=+1$ and the other where $u(t)=-1$. Next, divide the area according to whether the state $\mathbf{x}(t)$ is in the interior or exterior of the circular target set. Finally, divide the region acording to whether $|x_1| < R_o$ or $|x_1| > R_o$. The control system must sense where the state $\mathbf{x}(t)$ is and respond by producing $V_{MAX}u(t)$. This can be done by applying different control laws for the various regions just described and then using combinational logic circuitry to determine the final value of $u(t)$. When all the math has been sorted out the control can be stated as

$$u(t) = \begin{cases} \text{sign}(x_2) \text{ if } r^2 < R_o^2 \\ -\text{sign}(x_2) \text{ if } |x_1| < R_o \text{ and } r^2 > R_o^2 \\ -\text{sign}\left[x_2 + \text{sign}(x_1)\sqrt{(|x_1|-R_o)(2V_{MAX}+R_o-|x_1|)} \right] \\ \qquad \text{if } |x_1| > R_o \text{ and } r^2 > R_o^2 \end{cases} \tag{2.58}$$

where r is the amplitude of the time varying signal given by

$$r^2(t) = x_1^2 + x_2^2 \tag{2.59}$$

The reason why $r^2(t)$ is used in the above expression is made clear in

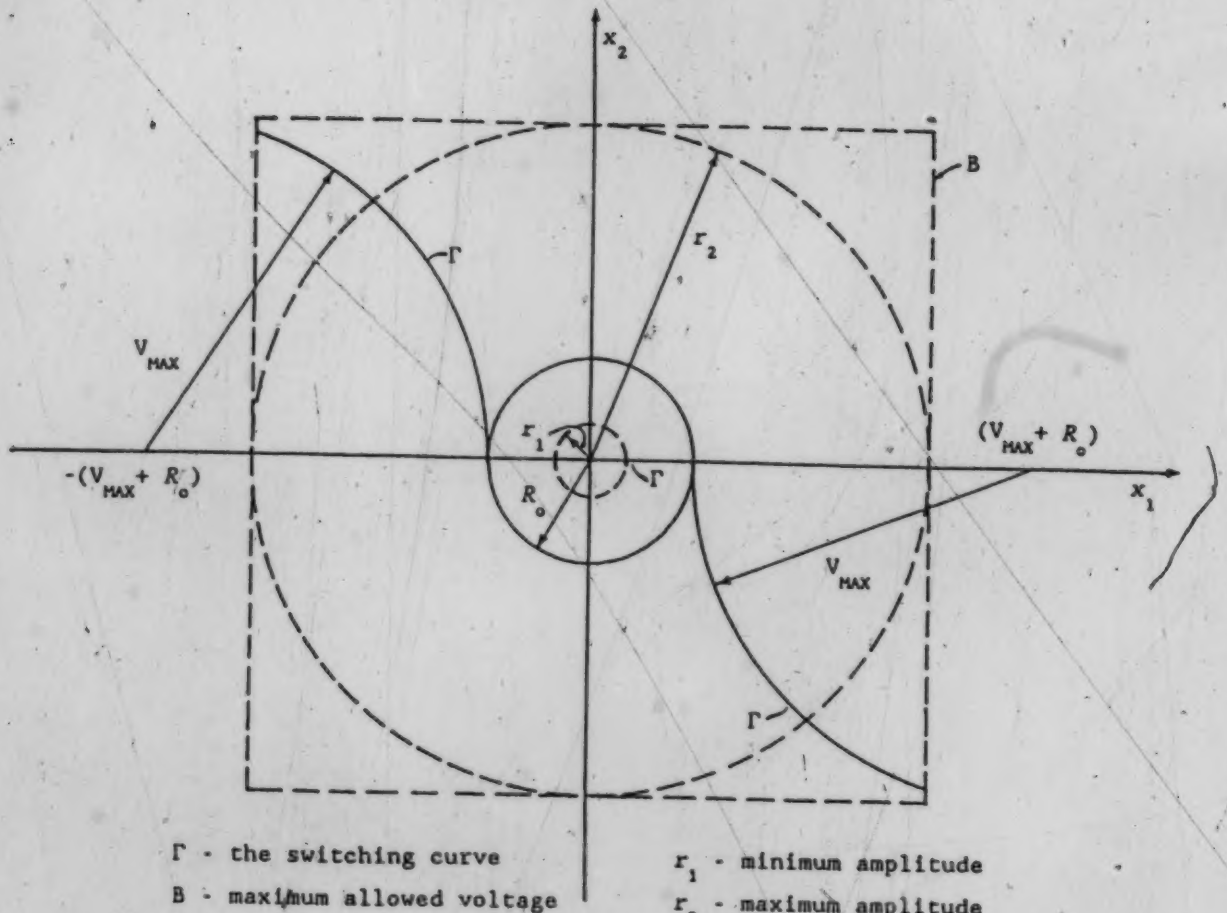

FIG. 2.13 THE SIMPLIFIED SWITCHING CURVE

the section covering the tracking regulator.

This proposed control law is the basis for the circuit which was built and is described in chapter 3. In order to obtain the control law information about the applicable region of the phase plane was exploited to simplify the nature of the control and thus enable the circuit realization. Without the simplification the circuit would have been virtually impossible to build. Yet, the simplification only introduces an error when the initial amplitude is less than the desired one. Therefore, very little performance was sacrificed to find a circuit that could be built.

2.4 SYNTHESIS OF THE OPTIMAL TRACKING REGULATOR

The time-optimal control forces the system to the desired amplitude in minimum time. What then? At $t=t_f$, $u(t)=0$ and presumably the system continues to oscillate without assistance - at least according to the mathematics. In any physical system noise and component tolerances will disturb the system causing it to deviate from the desired amplitude. What is needed is a control that will maintain the desired amplitude during steady state operation. The design of such a control is the objective of this section.

The discussion begins by transforming the system of

$$\dot{x} = Ax \tag{2.60}$$

into the polar coordinates

$$\begin{bmatrix} \dot{r} \\ \dot{\theta} \end{bmatrix} = \begin{bmatrix} 0 \\ \beta \end{bmatrix} \tag{2.61}$$

By doing so the amplitude and phase have been separated and the control can be applied strictly to the amplitude. It also simplifies the solution of the optimal control since only a one dimensional system occurs. The form of the differential equation is

$$\dot{r} = bu \tag{2.62}$$

where $u(t)$ is to be determined.

What should the performance index be? There are two possibilities. The goal is to force $r(t)$ to be R_o and should the system be disturbed the goal is to resist the change. The more circular the actual orbit is the fewer the harmonics present in the output signal. Begin by assuming $r(t) \neq R_o$; take the difference and then derive a positive quantity called $e(t)$ such that

$$e(t) = [r(t) - R_o]^2 \tag{2.63}$$

$e(t)$ is the error signal which represents the degree of deviation of the actual amplitude from the desired signal.

It is apparent that $e(t)$ must be minimized over time. The control must also be smooth and continuous. If a discontinuous control were designed such as the time-optimal control it would introduce its own harmonics into the signal, an obviously undesirable result. The control effort must also be minimized. To do that $u^2(t)$ must be minimized over time. So the performance index takes the form

$$J_1 = \lim_{t_f \to \infty} \frac{1}{2} \int_o^{t_f} q[r(t) - R_o]^2 + u^2(t)dt \tag{2.64}$$

Now the results of section 2.1 can be applied. The Hamiltonian (2.7) becomes

$$H = \frac{q[r(t) - R_o]^2}{2} + \frac{u^2(t)}{2} + p(t)bu(t) \tag{2.65}$$

There are no bounds on $u(t)$ therefore equation (2.11) is used so that

$$\frac{\partial H}{\partial u} = 0 = u(t) + p(t)b \tag{2.66}$$

which becomes

$$u(t) = -p(t)b \tag{2.67}$$

Applying (2.10) gives

$$\frac{\partial H}{\partial r} = q(r(t) - R_o) = -\dot{p} \tag{2.68}$$

Combining the results of equations (2.62), (2.67) and (2.68) gives a second order differential equation in r, namely,

$$\ddot{r} = b^2 q(r - R_o) \tag{2.69}$$

and $u(t)$ in terms of r is

$$u(t) = \frac{\dot{r}}{b} \tag{2.70}$$

To solve (2.69) let

$$\dot{r} = \frac{dr}{dt} = v \tag{2.71}$$

then

$$\ddot{r} = \frac{dv}{dt} = \frac{dv}{dr} \cdot \frac{dr}{dt} = \frac{dv}{dr} v \tag{2.72}$$

and apply (2.72) to (2.69) to give

$$vdv = b^2 q(r - R_o)dr \tag{2.73}$$

Solving for v gives

$$v(t) = \dot{r}(t) = \pm\sqrt{b^2 q(r - R_o)^2 + c_1} \tag{2.74}$$

As $t \to \infty$, $r(t)$ approaches R_o, therefore, $\dot{r}(t) \to 0$. With this information the constant of integration c_1 is determined to be zero and (2.74) is

$$\dot{r}(t) = \pm b\sqrt{q}\,(r - R_o) \tag{2.75}$$

If $r(t) > R_o$, $r(t)$ must decrease, therefore it is reasonable to require $\dot{r}(t) < 0$ so the negative square root is taken, hence

$$\dot{r}(t) = -b\sqrt{q}\,(r - R_o) \tag{2.76}$$

Equation (2.76) is easily solved to give

$$r(t) = ke^{-b\sqrt{q}\,t} + R_o \tag{2.77}$$

where

$$k = r_o - R_o \tag{2.78}$$

and $u(t)$ is

$$u(t) = -\sqrt{q}\,(r - R_o) \tag{2.79}$$

Equation (2.79) looks simple enough to implement and indeed it is. However the circuitry must derive $r(t)$ from $x_1(t)$ and $x_2(t)$. Since

$$r(t) = \sqrt{x_1^2(t) + x_2^2(t)} \tag{2.80}$$

can the square root operation be avoided? Such a question motivated

the change in the definition of $e(t)$ to

$$e(t) = \left[r^2(t) - R_o^2\right]^2 \tag{2.81}$$

since $r^2(t)$ is easier to derive from the circuitry than $r(t)$. The new performance index is

$$J_2 = \lim_{t_f \to \infty} \int_o^{t_f} \frac{q}{4} \left[r^2(t) - R_o^2\right]^2 + \frac{1}{2} u^2(t)dt \tag{2.82}$$

and the differential equation is

$$\dot{r} = b^2 qr(r^2 - R_o^2) \tag{2.83}$$

The same procedure can be applied as before, however, the results are slightly different. The control $u(t)$ is

$$u(t) = -\sqrt{q}\,(r^2 - R_o^2) \tag{2.84}$$

and $r(t)$ has the solution

$$r(t) = R_o \left[\frac{1 + ke^{-2bR_o\sqrt{q}\,t}}{1 - ke^{-2bR_o\sqrt{q}\,t}}\right] \tag{2.85}$$

where k is

$$k = \frac{r_o - R_o}{r_o + R_o} \tag{2.86}$$

The results can now be transformed back into the original coordinate system. Starting with equation (2.62) the differential system becomes

$$\begin{bmatrix} \dot{x}_1 \\ \dot{x}_2 \end{bmatrix} = \begin{bmatrix} \dfrac{bu}{\sqrt{x_1^2 + x_2^2}} & \beta \\ -\beta & \dfrac{bu}{\sqrt{x_1^2 + x_2^2}} \end{bmatrix} \begin{bmatrix} x_1 \\ x_2 \end{bmatrix} \tag{2.87}$$

Now either value for $u(t)$ can be substituted into equation (2.87). For the first performance index, letting $r = \sqrt{x_1^2 + x_2^2}$, (2.87) becomes

$$\begin{bmatrix} \dot{x}_1 \\ \dot{x}_2 \end{bmatrix} = \begin{bmatrix} \dfrac{-b\sqrt{q}\,(r - R_o)}{r} & \beta \\ -\beta & \dfrac{-b\sqrt{q}\,(r - R_o)}{r} \end{bmatrix} \begin{bmatrix} x_1 \\ x_2 \end{bmatrix} \qquad (2.88)$$

and for the second performance index

$$\begin{bmatrix} \dot{x}_1 \\ \dot{x}_2 \end{bmatrix} = \begin{bmatrix} \dfrac{-b\sqrt{q}\,(r^2 - R_o^2)}{r} & \beta \\ -\beta & \dfrac{-b\sqrt{q}\,(r^2 - R_o^2)}{r} \end{bmatrix} \begin{bmatrix} x_1 \\ x_2 \end{bmatrix} \qquad (2.89)$$

Figure 2.14 shows the resulting trajectories for the two performance indices given $\beta = 10b\sqrt{q} = 1$, $R_o = 5$ and $r_o = 0$. It is clear that for J_2, the resulting amplitude approaches R_o far more quickly. The difference between the two is minor, yet the performance is substantially different. Obviously, the control based on the second performance index is preferrable.

With the two possible controls derived, equation (2.87) reveals a problem. Namely, the expression

$$\frac{bu}{\sqrt{x_1^2 + x_2^2}}$$

is hard to implement. It is possible to implement but performing the square root function and especially division produces the possibility of an unacceptable error in the control signal. Also, what happens if $r(t) = 0$? As with the time optimal control a sub-optimal controller is more feasible than the optimal one. However, the optimal control can still be used as a standard and may suggest a possible sub-optimal design. The idea will be investigated in the next section.

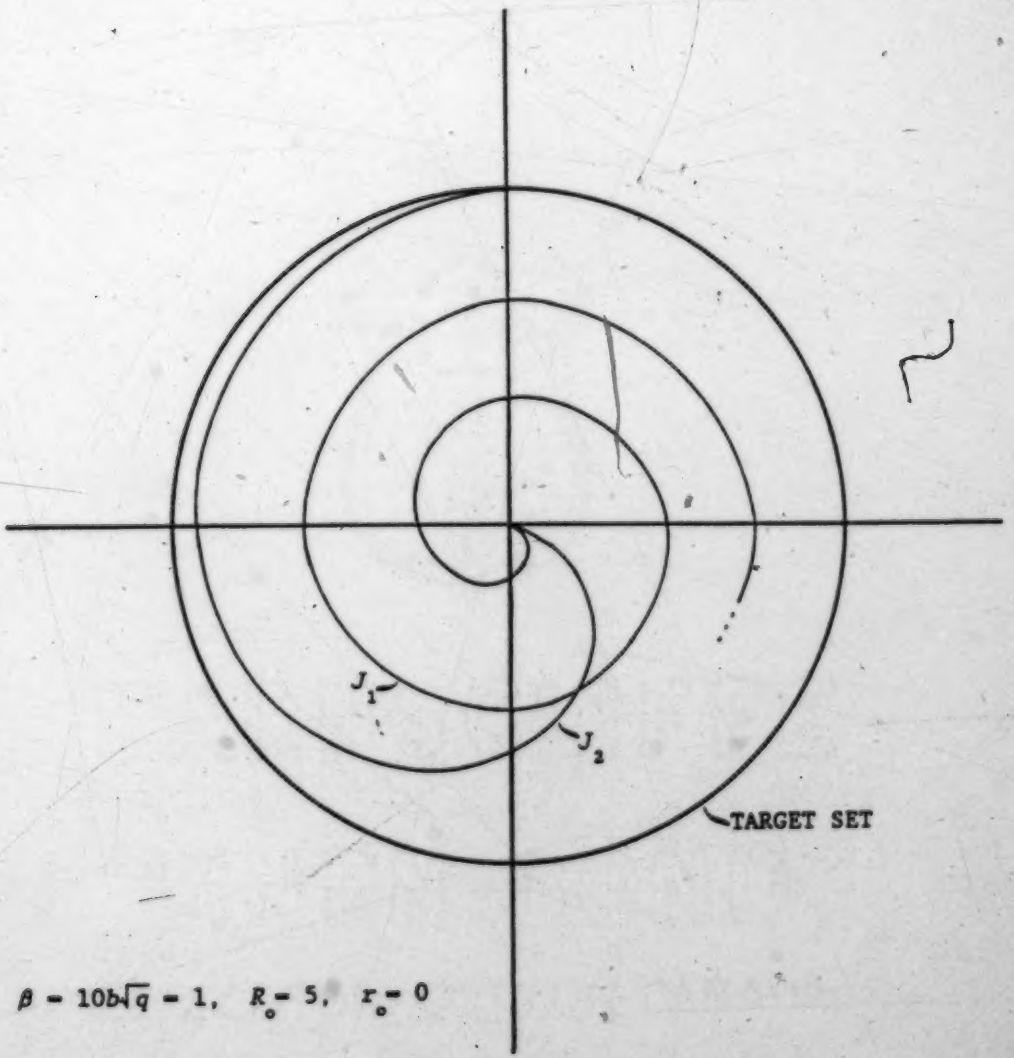

$\beta = 10b\sqrt{q} = 1, \quad R_o = 5, \quad r_o = 0$

FIG. 2.14 THE OPTIMAL TRAJECTORIES FOR THE TWO PERFORMANCE INDICES

2.5 A SUB-OPTIMAL TRACKING REGULATOR

It has been pointed out already that the optimal tracking regulators have a serious problem when it comes to implementation. This section will propose a different tracking regulator. It is not optimal in the perfect sense but, as the circuit demonstrates, it works. It actually has been around for some time (see Herpy [16] and Vidyasagar [17]). The control is obtained by manipulating the control expression so that there is no division by r in the final form of the equations.

Consider the control expression for the second performance index.

$$u(t) = -\sqrt{q}\,(r^2 - R_o^2) \tag{2.90}$$

Why not multiply (2.90) by $r(t)$? Then, when the system is transformed into Cartesian coordinates, the $r(t)$ in the numerator will cancel with the $r(t)$ in the denominator. Note that the control for the second index was chosen over the first because it is easier to synthesize $r^2(t)$ than it is $r(t)$. The resulting control is now given as

$$u(t) = \sqrt{q}\; r(r^2 - R_o^2) \tag{2.91}$$

In the Cartesian system the control $u(t)$ becomes

$$\begin{bmatrix} u_1 \\ u_2 \end{bmatrix} = -\sqrt{q}\;(r^2 - R_o^2)\begin{bmatrix} x_1 \\ x_2 \end{bmatrix} \tag{2.92}$$

The differential equations are

$$\begin{bmatrix} \dot{x}_1 \\ \dot{x}_2 \end{bmatrix} = \begin{bmatrix} -b\sqrt{q}\,(r^2 - R_o^2) & \beta \\ -\beta & -b\sqrt{q}\,(r^2 - R_o^2) \end{bmatrix}\begin{bmatrix} x_1 \\ x_2 \end{bmatrix} \tag{2.93}$$

Equations (2.93) are the basis for the circuit design of the tracking

regulator that is discussed in chapter 3[2].

What kind of performance does this new system have? Does it even work as a controller? Well, it does control the amplitude and the system even has a closed form solution. In terms of $r(t)$, the differential equation is

$$\dot{r} = -b\sqrt{q}\, r(r^2 - R_o^2) \tag{2.94}$$

and the solution to the system is

$$r(t) = \frac{R_o}{\sqrt{1 - ke^{-2R_o^2 b\sqrt{q}\, t}}} \tag{2.95}$$

$$\theta(t) = \beta t + \theta_o$$

where

$$k = \frac{r_o - R_o}{r_o^2}, \quad r_o \neq 0 \tag{2.96}$$

The values for x_1 and x_2 can be found from

$$\begin{bmatrix} x_1 \\ x_2 \end{bmatrix} = r(t) \begin{bmatrix} \sin\theta(t) \\ \cos\theta(t) \end{bmatrix} \tag{2.97}$$

The performance of the system can be compared in Fig. 2.15 where $r(t)$ has been plotted versus time. Note that the rate of convergence is faster for the proposed control than for the optimal control. One might expect the optimal control to perform better than the

---

[2] It is obvious that (2.90) is not completely expressed in Cartesian coordinates. In fact the equation is a mixture of both polar and Cartesian variables. The reason is not simply the need for a compact expression but rather this is the way the circuit was conceptualized. That is, circuitry was designed based on $r(t)$ rather than on $x_1(t)$ and $x_2(t)$ when it made sense to do so and the converse is also true.

sub-optimal one. It does in terms of its performance index but not necessarily in terms of the rate of convergence to the desired trajectory. The expression chosen for J minimizes the error between the actual amplitude and the desired one, and the control effort. It is the second term, namely, the control effort, that is not minimized in the proposed controller and thus allows the system to converge more rapidly. However, if J were computed for the two systems the minimum value would be obtained for the optimal control chosen. What, in effect, is being said is that the J chosen for the problem was not the one that best described the design goals. It was not necessary to minimize the control effort, all that was required was that the control be "smooth" and provide a circular limit cycle so that the distortion products would be small. However, to have actually found a J that described these goals would have probably made the optimal control solution intractable or at the least an open loop control, neither of which would have helped in the design of the circuit. The approach that was used, though it did not provide the actual solution, did provide the insight into the problem that eventually led to the control chosen.

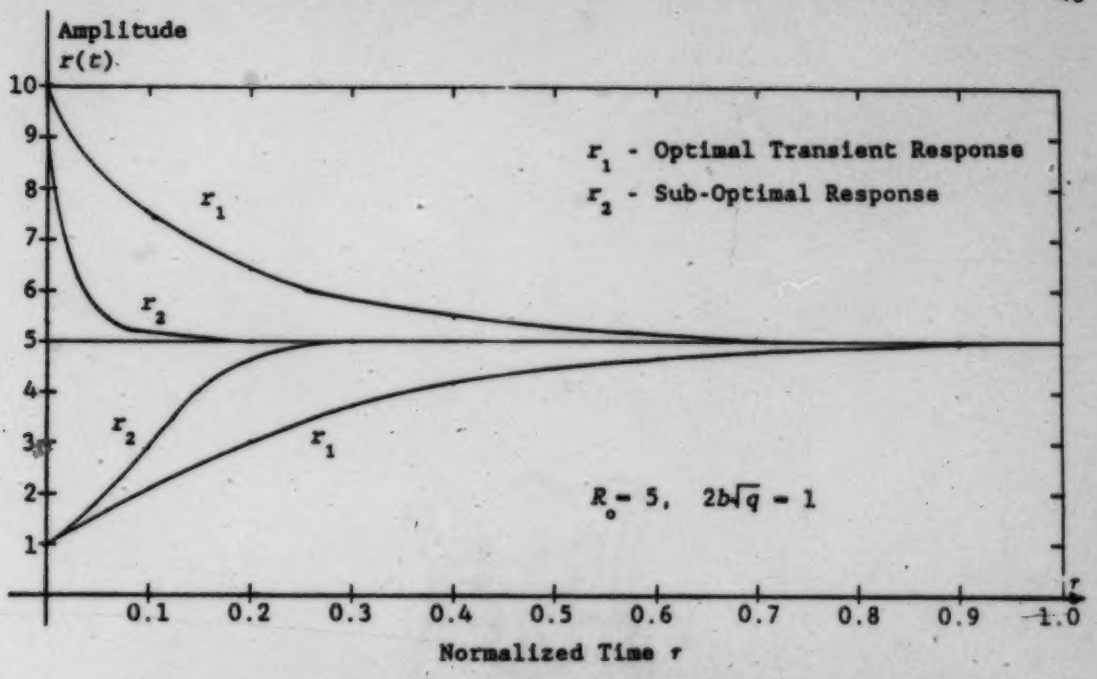

FIG. 2.15 THE TRANSIENT RESPONSE FOR THE OPTIMAL AND SUB-OPTIMAL CONTROLS

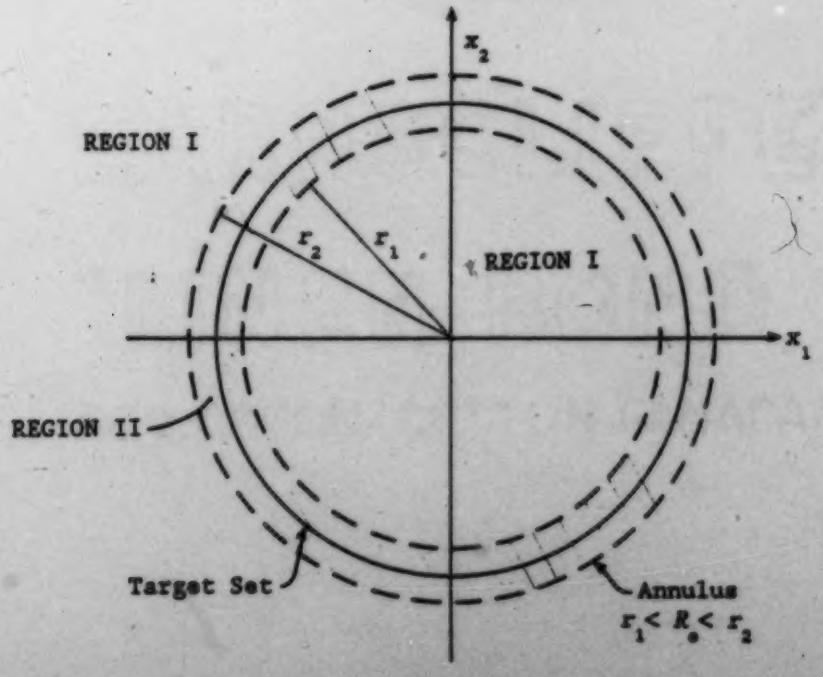

FIG. 2.16 THE REGION OF THE PHASE PLANE FOR WHICH STEADY STATE OPERATION IS DEFINED

2.6 A DUAL MODE CONTROLLER

So far, the control laws for the fast amplitude controller and the tracking regulator have been developed to the point where the circuits can be designed. However, the problem of how to switch from one control to the other has not yet been addressed. The purpose of this section is to solve that problem.

The problem can be defined as determining the two states of operation - namely, steady state and transitional behavior. The question is how does one determine one of these two conditions? The answer lies in the expression for the error between the actual amplitude and the desired one. The equation for the error is given as

$$e = r^2 - R_o^2 \qquad (2.98)$$

Ideally, when e is zero this would indicate steady state behavior and when e is other than zero this would be transitional behavior. This definition, however, is inadequate since the solution to the tracking regulator takes an infinite amount of time to reach steady state. The other consideration is that in a practical sense e will never be zero due to the non-idealities of the circuit. Therefore, the definition has to be changed to say that the steady state occurs when $|e|$ is small and when e is not small this will indicate that the fast controller should take over. Exactly what is meant by "small" will only be known when the circuit is built and some measure of the magnitude of e can be ascertained. Geometrically this can be viewed as an annular region defined over the circular target set. Whenever the state is outside the annular region this indicates transient behavior and inside steady state conditions would prevail (see Fig. 2.16). The width of the annulus should be variable to allow for variations in the error signal. This can easily be done with a window

comparator. The output from the comparator can then be used to switch control signals. The dual mode controller then determines which control should be applied to the oscillator and when it should be applied. It is a rather simple concept and presents no problems for the circut designer and thus the problem of switching is easily solved.

In this chapter three control systems have been designed each a sub-system of the overall control for the oscillator. The tracking regulator operates during steady state so that the control is smooth thereby introducing little distortion into the circuit. The fast amplitude control is based on the results of time optimal control theory. It is designed to operate during transitional periods when the amplitude is changing. The dual mode control, whose purpose is to switch between the two other controls, is the final control stage.

CHAPTER THREE: THE CIRCUIT IMPLEMENTATION

3.0 INTRODUCTION

The job is only half done when the control equations have been derived. The final half involves the designing and testing of the circuit. The chapter is divided into two main sections. The first discusses the design of the circuitry. This section is further broken down into subsections, each covering a particular sub-circuit. The other section covers the testing of the circuit and it is sub-divided into two parts. The first part deals with the distortion measurements and discusses the dominant harmonic frequencies and how they arise. Ways in which distortion can be reduced are considered. The final part covers the transient response measurements and ends the chapter.

3.1 CIRCUIT DESIGN

The design of the complete circuit begins by designing the various sub-circuits. An overview of the entire system and how the various sub-systems are interconnected is illustrated in Fig 3.1. The approach to the circuit design is the same as designing an analog computer which simulates the differential equations discussed in chapter 2. The outputs of the oscillator are the state variables v_1 and v_2. These voltages are the inputs to the tracking regulator and the fast amplitude controller. The voltage V_R is the reference voltage and represents the desired amplitude of oscillation. The outputs of the tracking are e_{1SS} and e_{2SS}, which are the steady state control signals for the oscillator, and v_e, which is the error signal representing the difference between the actual and the desired amplitudes. v_e is an input for the dual mode controller and the fast amplitude controller. The dual mode controller uses v_e to determine if steady state has been achieved and the fast amplitude controller uses it to determine whether the amplitude must be increased or decreased. The fast amplitude controller has only one output, e_{2TR}, which is the transient control signal for the oscillator. To ensure that the control input e_{1C} is not undefined during transitions e_{1TR} is connected to ground. With the input and output signals defined and their functions determined the design of the circuits can begin, starting with the oscillator.

3.1.1 The Oscillator Circuit Design

The design of the oscillator circuit is considered in this section along with some of the problems and the approximations to the

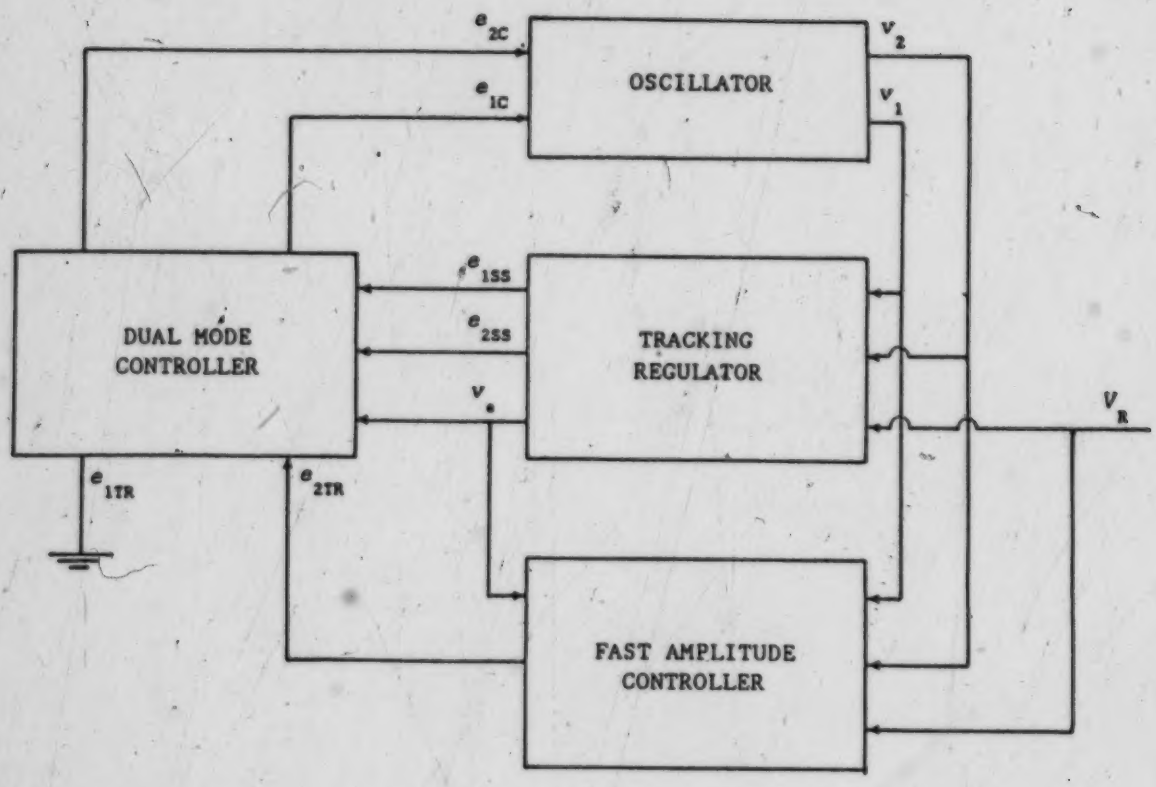

FIG. 3.1 SYSTEM OVERVIEW

ideal that are to be encountered. Some of the problems to be discussed are offset compensation, eigenvalues with non-zero real parts, the effect of component tolerance on the determination of the frequency, slew rate limitations and supply current limitations. The section begins by explaining the design of the state variable oscillator.

The oscillator comprises two integrators where the first feeds directly into the second and the second one feeds into the first after its signal has been inverted. The outputs of the two integrators are sinusoids that are 90° out of phase. Figure 3.2 shows the actual circuit for the oscillator. To avoid inverting the voltage v_2 the op-amp A1a is configured as a differential integrator thus reducing the number of op-amps required. The op-amps chosen for the circuit were Precision Monolithics OP-227GY [18]. This IC has two matched ampifiers on the same chip producing the advantage that they will track each other thermally. Each output is buffered to prevent any possible loading by the control circuitry because the voltage signals v_1 and v_2 feed into several points in the control circuitry.

The challenge of designing an integrator is in dealing with the bias and offset currents of the op-amp. The first step is to cancel the bias currents. This was achieved by configuring amplifier A1a as a differential integrator and by adding bias compensation resistor R_6 to A1b. Then the resistances and capacitances were chosen so that the signal currents were large with respect to the offset currents. This does not solve the problem completely but it helps.

An ideal integrator has infinite gain at dc and no offset current to irk the designer. However, an actual op-amp has finite gain at dc

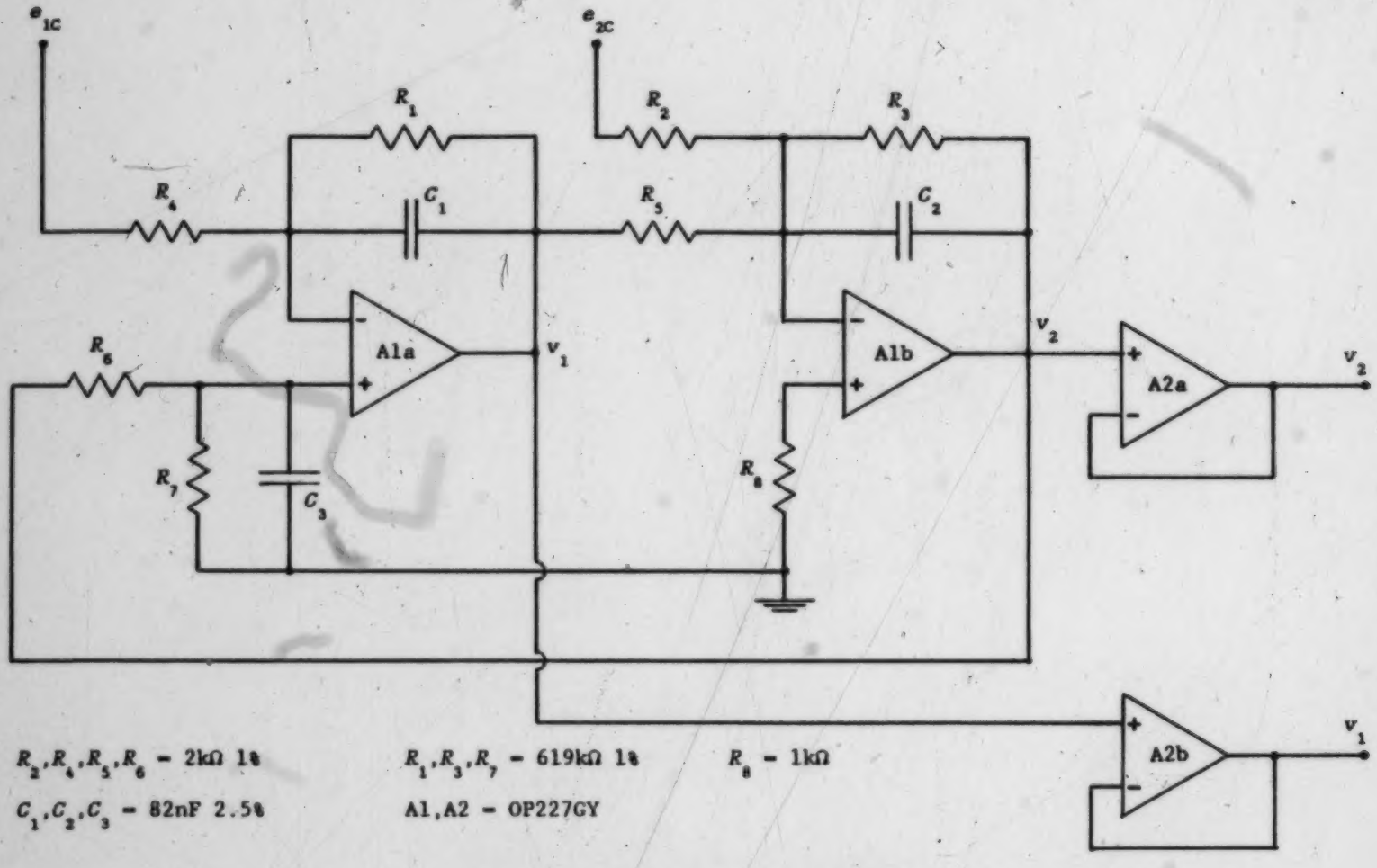

R_2, R_4, R_5, R_6 - 2kΩ 1%

C_1, C_2, C_3 - 82nF 2.5%

R_1, R_3, R_7 - 619kΩ 1%

A1, A2 - OP227GY

R_8 - 1kΩ

FIG 3.2 OSCILLATOR CIRCUIT DESIGN

which is large enough to cause the amplifier to saturate due to the integration of the offset current. To avoid this the dc gain was reduced by the addition of R_1 and R_3. For the values shown in Fig. 3.2 the dc gain was 50 dB and the corner frequency was 3 Hz. This ensured that from 10 Hz to 100 kHz the amplifier still remained an integrator.

The addition of R_1 and R_3 in the feedback path of each amplifier presents another problem. Amplifier A1b is configured as a summing integrator. That is, it sums and integrates the two voltages v_1 and e_{2C}. Now let $R_2 = R_4 = R_5 = R_6 = R_i$, let $R_1 = R_3 = R_7 = R_f$ and let $C_1 = C_2 = C_3 = C$. The expression for v_2 is

$$\dot{v}_2 = -\beta v_1 - \alpha v_2 - \beta e_{2C} \tag{3.1}$$

where $\beta = 1/R_iC$ and $\alpha = 1/R_fC$. Because A1a is configured as a differential integrator the expression for v_1 is slightly different; namely,

$$\dot{v}_1 = -\alpha v_1 + \beta v_2 - \beta e_{1C} \tag{3.2}$$

If (3.1) and (3.2) are put in vector form then the coefficient matrix is

$$A = \begin{bmatrix} -\alpha & \beta \\ -\beta & -\alpha \end{bmatrix} \tag{3.3}$$

Compare (3.3) with (2.18). Note that (3.3) has nonzero values on the diagonal; this is due to the finite gain that was required for the offset currents. The result is that the eigenvalues for the harmonic oscillator now have negative real parts. The only thing that can be done is to make α as small as possible. For the circuit values given $\alpha = 19.7$ rad/sec whereas $\beta = 6097.6$ rad/sec. Since β is roughly 300 times larger than α the effects should be small enough to enable the

control to compensate.

The frequency of oscillation is determined by the passive components R_1 and C. The nominal design frequency was 1000 Hz. With the values of the components available, the actual design frequency was 970 Hz. If the tolerances indicated in Fig. 3.2 are taken into account, the oscillation frequency can be expected to be anywhere between 937.4 and 1005.4 Hz. The actual frequency of oscillation was 975 Hz. Since the frequency is determined solely by passive components the frequency stability is determined by the stability of the passive components. The variation of frequency with temperature is given as

$$S_T^f = -S_T^R - S_T^C \tag{3.4}$$

where S_T^f is the frequency sensitivity defined as

$$S_T^f = \frac{1}{\beta}\frac{d\beta}{dT} \tag{3.5}.$$

Since the temperature coefficient of the resistors is 100 ppm/°C and 180 ppm/°C for the capacitors the value of S_T^f is -280 ppm/°C. The only way to improve on this figure is buy better components or to obtain capacitors with negative temperature coefficients such that they cancel with the resistors' positive ones.

Any op-amp has limitations. Two limitations which concern the design of the oscillator are slew rate and maximum supply current. Neither of these is a concern when the oscillator is operating in the steady state since the frequency of oscillation is low enough. However, when the fast amplitude control (FAC) is applied the situation changes. In order to ensure that neither of the limits were

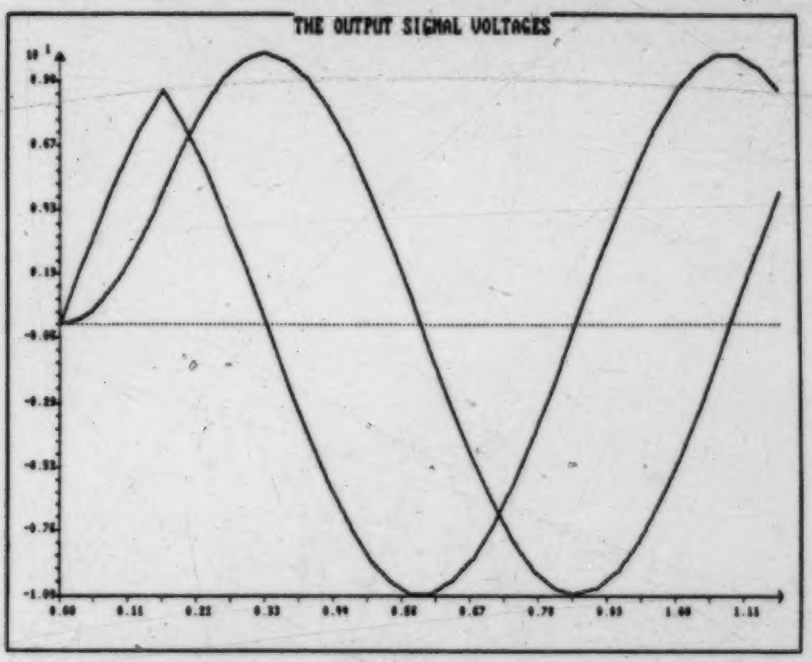

a) STEP-UP IN AMPLITUDE FROM 0 TO 10 VOLTS

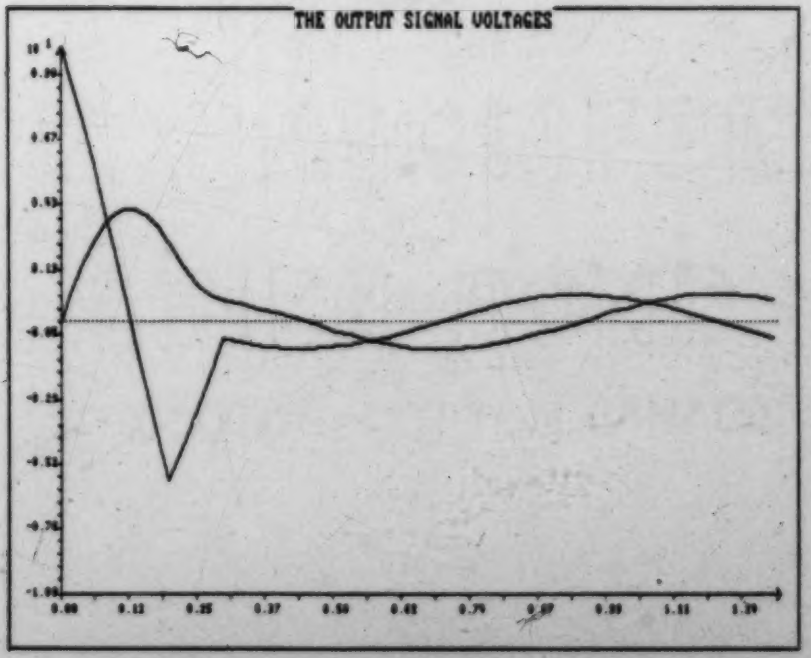

b) STEP-DOWN IN AMPLITUDE FROM 10 TO 1 VOLT

FIG. 3.3 OUTPUT VOLTAGES FOR A STEP-UP AND A STEP-DOWN IN AMPLITUDE

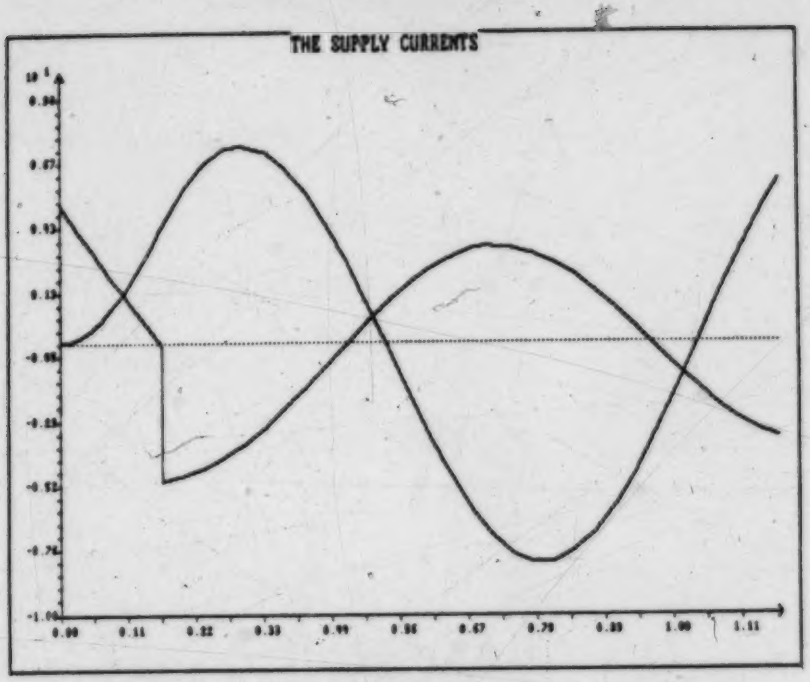

a) STEP-UP IN AMPLITUDE FROM 0 TO 10 VOLTS

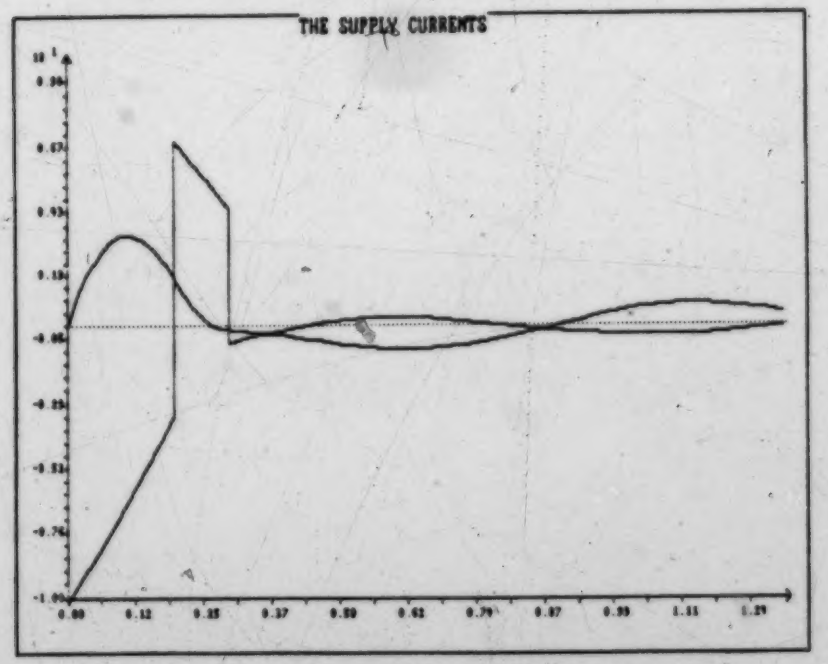

b) STEP-DOWN IN AMPLITUDE FROM 10 TO 1 VOLT

FIG. 3.4 OP-AMP SUPPLY CURRENTS

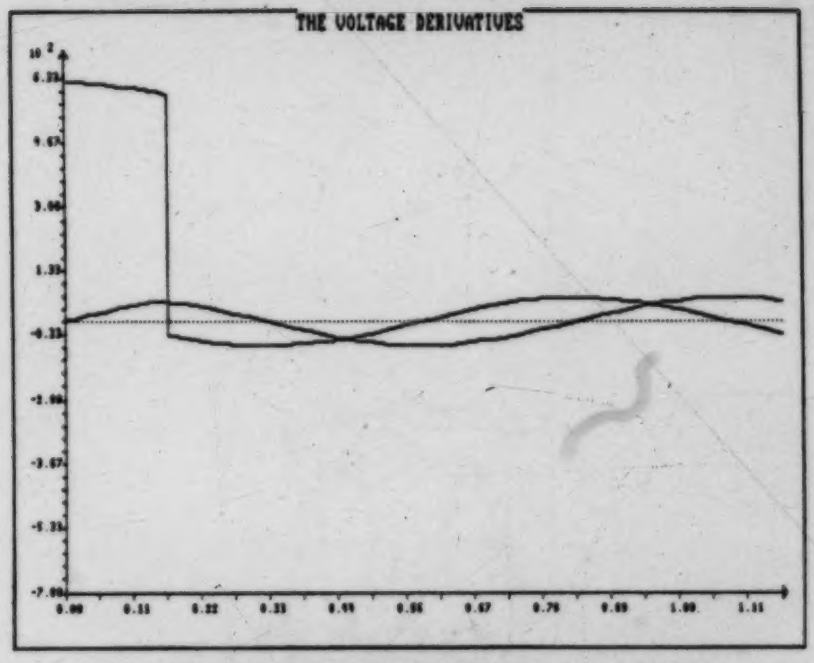

a) STEP-UP IN AMPLITUDE FROM 0 TO 10 VOLTS

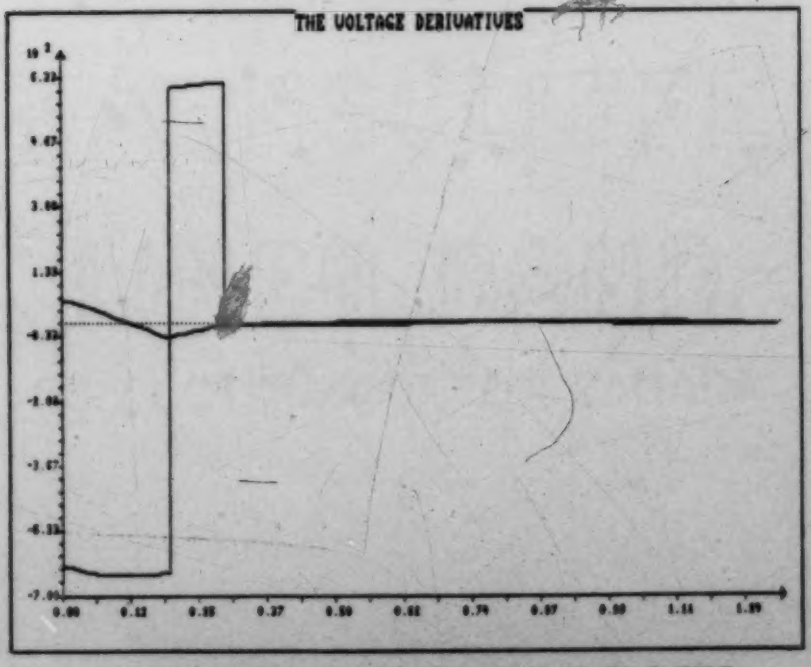

b) STEP-DOWN IN AMPLITUDE FROM 10 TO 1 VOLT

FIG. 3.5 OUTPUT VOLTAGE DERIVATIVES

exceeded a computer simulation, shown in Figs. 3.3, 3.4 and 3.5, was done. The program was written in Pascal and run on a PC. The results, which can be seen in the figures, indicates that the maximum voltage derivative that could be expected was -0.65V/μsec for $\dot{v}_2$ and the maximum current was -10.20mA for Alb. The data sheet for the OP-227 indicates that the slew rate is 2.8V/μsec and the maximum current is 50mA. So there is little need for concern at this oscillation frequency; however, if the need for a higher frequency was required then different op-amps would be required. The other point that arises from these results is that the circuit does not place big demands on Ala. It is possible, therefore, that Ala could be a more economical device with inferior performance specifications.

3.1.2 The Tracking Regulator

When the oscillator reaches steady state operation, as determined by the dual mode controller (DMC), the tracking regulator assumes responsiblity for controlling the amplitude. The circuitry which performs this function is shown in Fig. 3.6. This circuit generates the electrical analog of the signals $u_1(t)$ and $u_2(t)$ described in the equation (2.92). In addition another output is added which is proportional to the error signal e defined in (2.98). This signal, rather than being an input to the oscillator, is an input for the DMC and the fast amplitude controller (FAC).

The key building block of the tracking regulator is the multiplier. The multipier circuit is made up of two ICs. The MC1594 is a four quadrant multiplier [17]. The output of this multiplier is a current; in order to convert this current to a voltage a TL071C

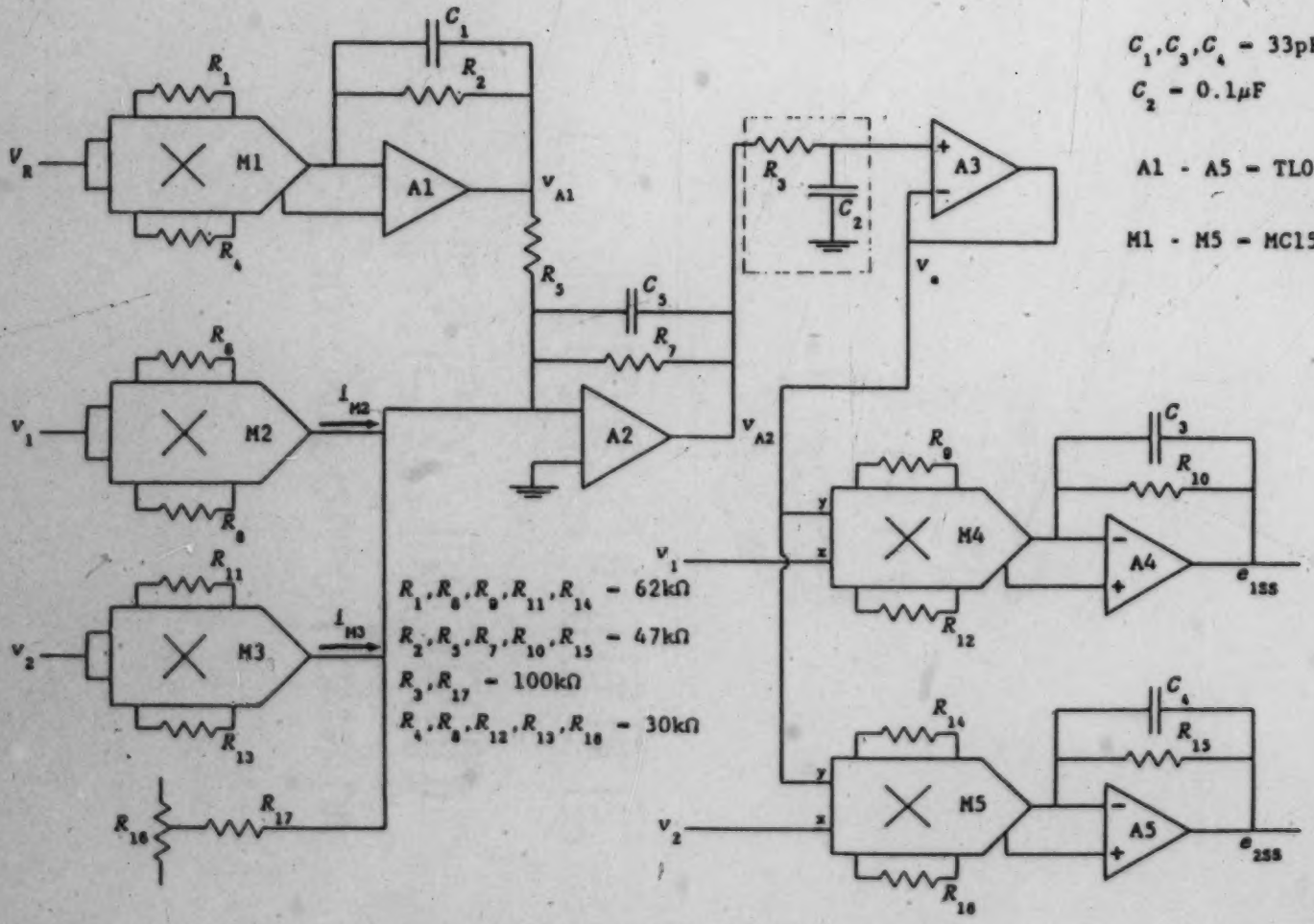

FIG. 3.6 TRACKING REGULATOR CIRCUIT DESIGN

op-amp is used as a curent to voltage converter [18]. The M1-A1 combination represents the basic multiplier circuit used and all remaining multiplier circuits are configured similarly. To aid the discussion consider the following definitions:

$$R_1 = R_6 = R_9 = R_{11} = R_{14} = R_X$$

$$R_4 = R_8 = R_{12} = R_{13} = R_{18} = R_Y$$

$$R_2 = R_5 = R_7 = R_{10} = R_{15} = R_L$$

$$C_1 = C_3 = C_4 = C_5 = C_C.$$

Since the MC1594 allows a maximum input voltage magnitude of 10V on both inputs scaling is required since it would be impossible for the output to reach 100V. Typically, a scaling factor of 1/10 is used so that the output is restricted to 10V. There are, however, two scaling factors which are pertinent. The first is related to just the multiplier and it is designated as K_1. K_1 relates the voltage inputs to the current output such that the expression for the current is

$$i_o = K_1 v_X v_Y \qquad (3.6)$$

K_1 in terms of the circuit components is given by (3.7).

$$K_1 = \frac{2}{R_X R_Y I_B} \qquad (3.7)$$

I_B is the bias current of the MC1594. The bias current is normally set by a resistor which is not shown in the figure. For information on biasing and offset nulling see the Motorola data book [17]. The second scaling factor is related to the multiplier op-amp combination and is called K. The expression for the voltage at the output of the op-amp is given by (3.8).

$$v_o = -K\, v_X v_Y \qquad (3.8)$$

Note the inversion of the signal is due to the op-amp. K is given by

$$K = R_L K_1 = \frac{2R_L}{R_X R_Y I_B} \qquad (3.9).$$

Applying equation (3.8) to the M1-A1 combination the voltage at the output of A1 is

$$v_{A1} = -K V_R^2 \qquad (3.10)$$

where $K = 0.1\ V^{-1}$. Again, applying equation (3.8) to the final stage of the tracking regulator results in two outputs e_{1SS} and e_{2SS} which are given by

$$e_{1SS} = -K v_e v_1 \qquad (3.11)$$

$$e_{2SS} = -K v_e v_2 \qquad (3.12)$$

where v_e is the output of A3. All that remains of the circuit analysis is to determine the expression for v_e.

The key to making the circuit work is generating the analog of $r^2(t)$. This is accomplished by M2 and M3. In this case the signal of interest is a current rather than a voltage. M2 and M3 create a current that is proportional to the square of their input voltages. When these two currents are summed the output is the equivalent of $r^2(t)$. The expression is given as

$$i_S = i_{M2} + i_{M3} = K_1 v_1^2 + K_1 v_2^2 = K_1 (v_1^2 + v_2^2) \qquad (3.13)$$

The next step is to generate the difference between the actual amplitude given by (3.13) and the desired amplitude (3.10). To do this the voltage v_{A1} is converted to a current by R_5 and then summed with i_S by amplifier A2. The resulting output expression for A2 is

$$v_{A2} = -K \left[(v_1^2 + v_2^2) - V_R^2 \right] \qquad (3.14).$$

Under normal operating conditions $v_{A2} = v_e$ and thus (3.14) is the error signal of (2.98) except inverted and scaled.

The circuit in the dashed box represents optional circuitry. Two types of circuits were tried. One was a voltage divider which effectively decreases the gain of the control. The other was a low pass filter. The purpose was to test the effects on the oscillator's performance especially with regard to distortion. When the optional circuitry is present $v_{A2} = v_o$.

Multipliers like op-amps have offsets. Much of the offset circuitry is not shown because it follows the suggested circuits in [17]. However, R_{16}, R_{17} form a non-standard bias circuit. R_{16} is a potentiometer configured as a voltage divider and R_{17} converts this voltage to a current. The purpose is to null the offset currents of M2, M3 and A2.

Unlike op-amps multipliers have vide bandwidths and when combined with an op-amp instability becomes a real possibility. In order to ensure that the circuit doesn't oscillate a compensation capacitor C_c is added. Although these components are required they do not enter the expressions for the controls.

With the information given the expressions for the controls can now be stated.

$$e_{1SS} = -K v_o v_1 = aK^2\left[(v_1^2 + v_2^2) - V_R^2\right] \qquad (3.15)$$

$$e_{2SS} = -K v_o v_2 = aK^2\left[(v_1^2 + v_2^2) - V_R^2\right] \qquad (3.16)$$

The voltages e_{1SS} and e_{2SS} are proportional to $-u_1$ and $-u_2$ which is what is required by the oscillator circuit since the inverting integrators will change the sign of the controls. The constant a is included in the expression for when the optional circuitry is in place. However, if a frequency dependent network is inserted then

(3.15) and (3.16) no longer apply since the order of the differential system will increase. When a is determined by a simple voltage divider the designer has direct control over the quantity q. q is related to a by

$$q = aK^2 \qquad (3.17).$$

So when $a = 1$ $q = 0.01$ which may appear to be small but it turns out that the major source of distortion is caused by the control itself. Therefore, the smaller the control signal is the less distortion there will be. In fact, the circuit was tested with a $q = 0.0001$. Even though there was a small error in the amplitude the distortion was reduced another 20dB. Of course as q gets smaller the transient response of the regulator gets longer. However, it is of no concern since the fast amplitude controller takes care of the transient response. This concludes the discussion of the tracking regulator.

3.1.3 Dual Mode Controller Circuit Design

The dual mode controller (DMC) has a logic output that controls the state of an analog switch (see Fig. 3.7). The analog switch used is Siliconix's DG243 [19] which is a dual dpst complementary switch. Complementary meaning that when one switch is on the other is off according to the control signal. The design of the DMC centers on deriving the correct control signal. Mathematically the function can be stated as

$$e_{SWITCH} = \begin{cases} \text{TRUE or HIGH if } |v_e| \leq \Delta V \\ \text{FALSE or LOW if } |v_e| > \Delta V \end{cases} \qquad (3.18).$$

Equation (3.18) is realized with a window comparator. The window comparator is comprised of two op-amps. The first amplifier Ala

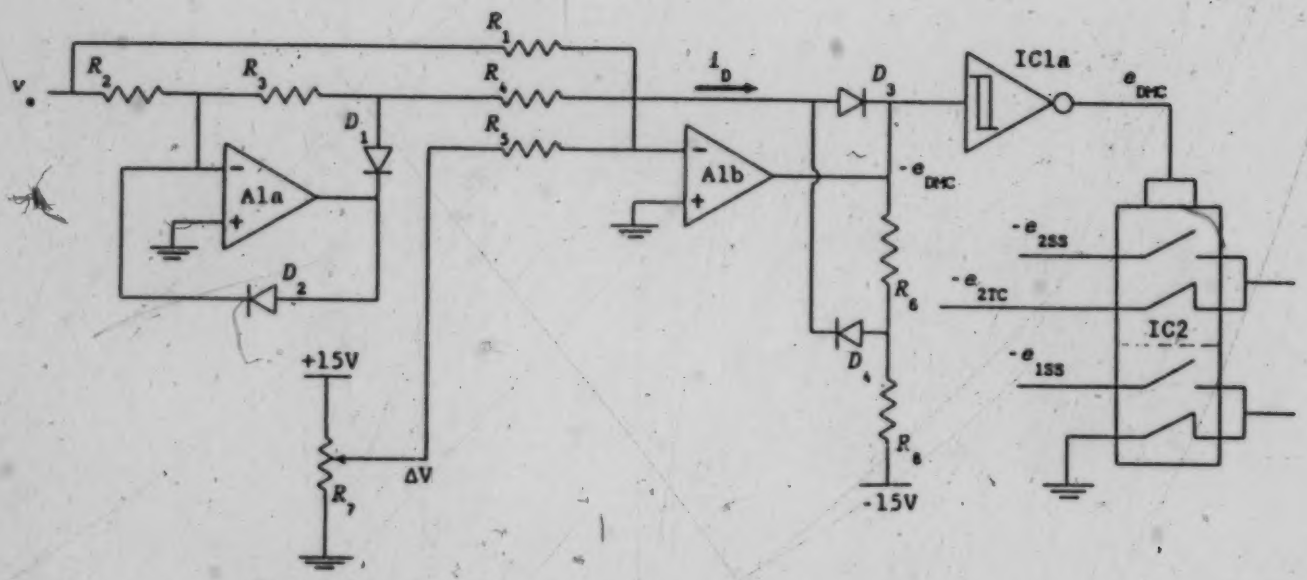

R_1, R_2, R_3, R_5 - 10kΩ R_4 - 5kΩ R_6 - 1kΩ R_7 - 10kΩ pot R_8 - 3kΩ
A1 - TL074 IC1 - 74HC14 IC2 - TL191

FIG. 3.7 DUAL MODE CONTROLLER CIRCUIT

functions as a half-wave rectifier. The second amplifier A1b works as an amplifier but the signal which it amplifies is switched according to the polarity of the summed currents at the inverting input of the op-amp. A1b should perhaps be called an attenuator since the gains are configured to be either zero or 1/3.

The circuit works in the following manner. When $v_o < 0$ diode D_2 is on and the output of A1a is zero. When $v_o > 0$ then D_1 is on and the output is now $-v_o$, since $R_2 = R_3$. Note that $R_1 = R_5 = 2R_4$. The polarity of the diode current i_D determines whether D_3 or D_4 is on and i_D is the sum of the currents at the input of A1b such that when $v_o > 0$ i_D is given by

$$i_D = \frac{-v_o}{R_4} + \frac{v_o}{R_1} + \frac{\Delta V}{R_5} = \frac{\Delta V - v_o}{R} \qquad (3.19)$$

where $R_1 = R_5 = R$ and $R_4 = R/2$. Diode D_3 will be on when $i_D \geq 0$. Applying this inequality to (3.19) the condition on v_o is

$$v_o \leq \Delta V \qquad (3.20).$$

It is easy to infer that D_4 is on when $v_o \geq \Delta V$. When D_3 is on the output of A1b is zero or logic low. When D_4 is on R_6 is connected in the feedback path and the output is 5V since the gain of R_6, R_8 and A1b is -1/3. The situation is slightly different when $v_o < 0$. The diode current i_D now becomes

$$i_D = \frac{v_o + \Delta V}{R} \qquad (3.21)$$

and the forward bias condition on D_3 gives the inequality for v_o as

$$v_o \geq -\Delta V \qquad (3.22).$$

The output of A1b can now be stated in terms of v_o and ΔV.

$$v_{A1b} = \begin{cases} 5V \text{ if } |v_e| \geq \Delta V \\ 0V \text{ if } -\Delta V \leq v_e \leq \Delta V \end{cases} \qquad (3.23)$$

Therefore, it is easy to see that the width of the window is $2\Delta V$ and since ΔV is variable, complete control over the DMC is achieved. Comparing (3.23) with (3.18), (3.23) represents the complement of the logic function required. This is why the output is followed by an inverter with hysteresis. It not only inverts the signal but sharpens switching transition as well as providing additional noise immunity.

3.1.4 Fast Amplitude Controller (FAC)

By far the most complicated circuit is the FAC. Part of the reason for this is the complex nature of the control law itself, stated in equation (2.58). The other reason is the synthesis of the switching curve which was illustrated in Fig. 2.13. This section will look at the circuitry that achieves this control law. The description divides the design into three parts. The first part deals with the circuit that produces a signal which simulates the semi-circular part of the switching curve in both the left and the right hand planes. A lot of signal processing is required and much of the circuitry of the FAC is devoted to producing just this function. The next part looks at the interface between the analog and the digital circuitry. The third and final part of this section discusses the logic circuitry and the switching of the control signals.

The first step in designing the FAC is simulating the switching curve. The most difficult parts of the switching curve to simulate are the two semi-circular portions shown in Fig. 2.13. The circuit

which does this is shown in Figs. 3.8 and 3.9. The function which the circuit realizes is

$$y = \sqrt{(|x_1| - R_o)(2V_{max} + R_o - |x_1|)} \qquad (3.24).$$

A quick study of the above expression reveals that the circuitry required should calculate the absolute value function, sum and subtract, determine the product and finally calculate the square root. Two absolute value circuits are used. Amplifiers A1a and A1b form one circuit and A1c and A1d form the other. The difference between the two is that one produces $|v_1|$ and the other $-|v_1|$. In every other way they are the same. The circuit surrounding A1a and A1b is very similar to the window comparator. Resistors 1,2,3 and 5 all have the same value and R_4 is half the value. The only difference between this circuit and the window comparator is the addition of R_5 and the absence of the second set of diodes. The analysis is very similar to that already covered. The voltages V_{MAX} and V_R are inverted and buffered by amplifiers A2a and A2b so that they can be used in the summing circuits of A3 and A4. The output of A4 is

$$v_{A4} = |v_1| - V_R \qquad (3.25)$$

since $R_{17} = R_{18} = R_{20}$. The summing circuit of A3 forms a sum proportional to $(2V_{MAX} + R_o - |x_1|)$. The actual output is scaled by 1/3 since there is the possiblity of a 30V output which the op-amp could never achieve. So the actual output of A3 is

$$v_{A3} = \frac{2V_{MAX} + V_R - |v_1|}{3} \qquad (3.26).$$

The two sums are fed into a multiplier circuit (M1-A5). Since multipliers have been discussed previously no more will be said except to say that the output of A5 is given by

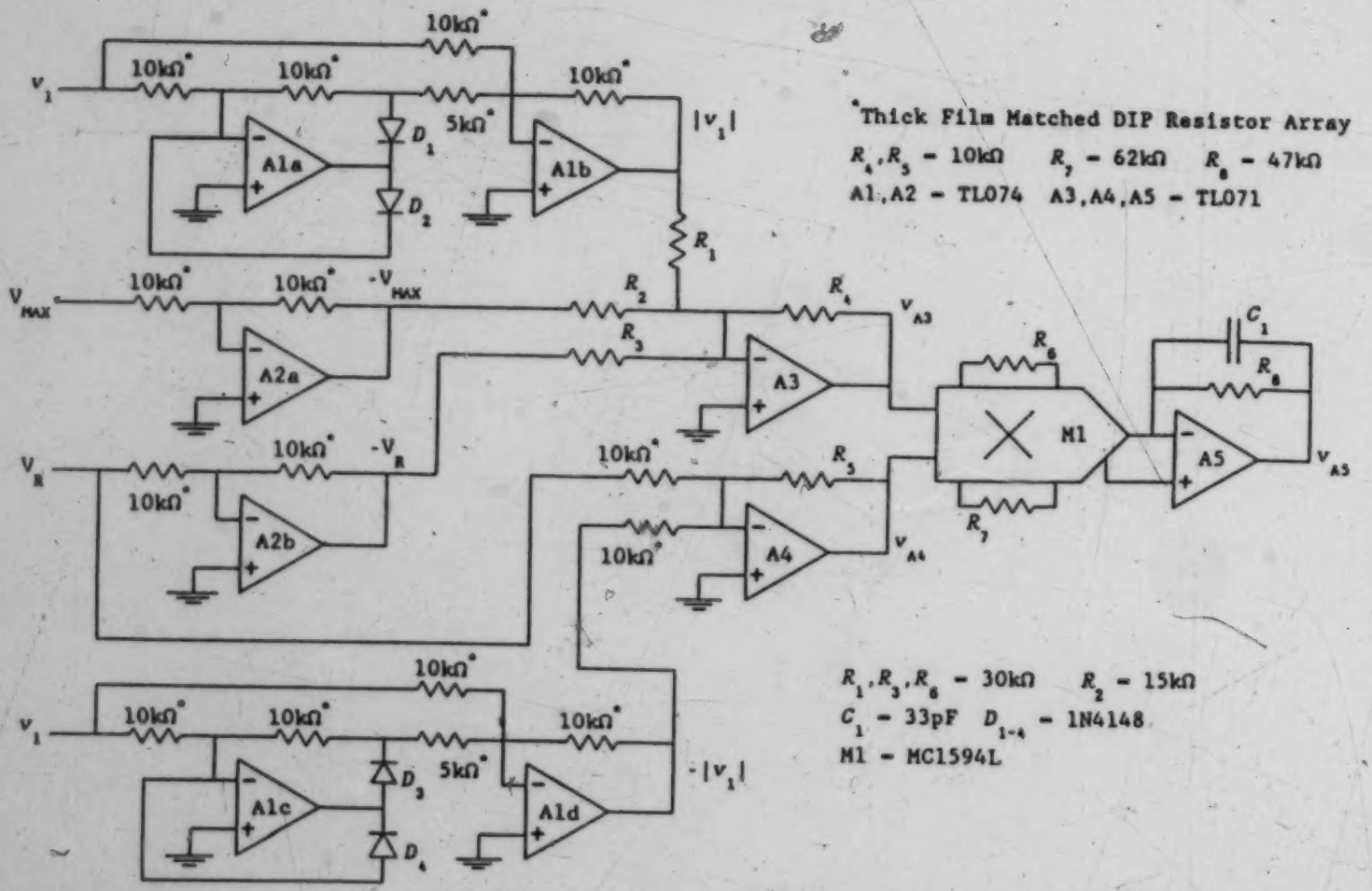

*Thick Film Matched DIP Resistor Array

R_4, R_5 - 10kΩ R_7 - 62kΩ R_8 - 47kΩ

A1, A2 - TL074 A3, A4, A5 - TL071

R_1, R_3, R_6 - 30kΩ R_2 - 15kΩ

C_1 - 33pF D_{1-4} - 1N4148

M1 - MC1594L

FIG. 3.8 FAST AMPLITUDE CONTROL CIRCUITRY

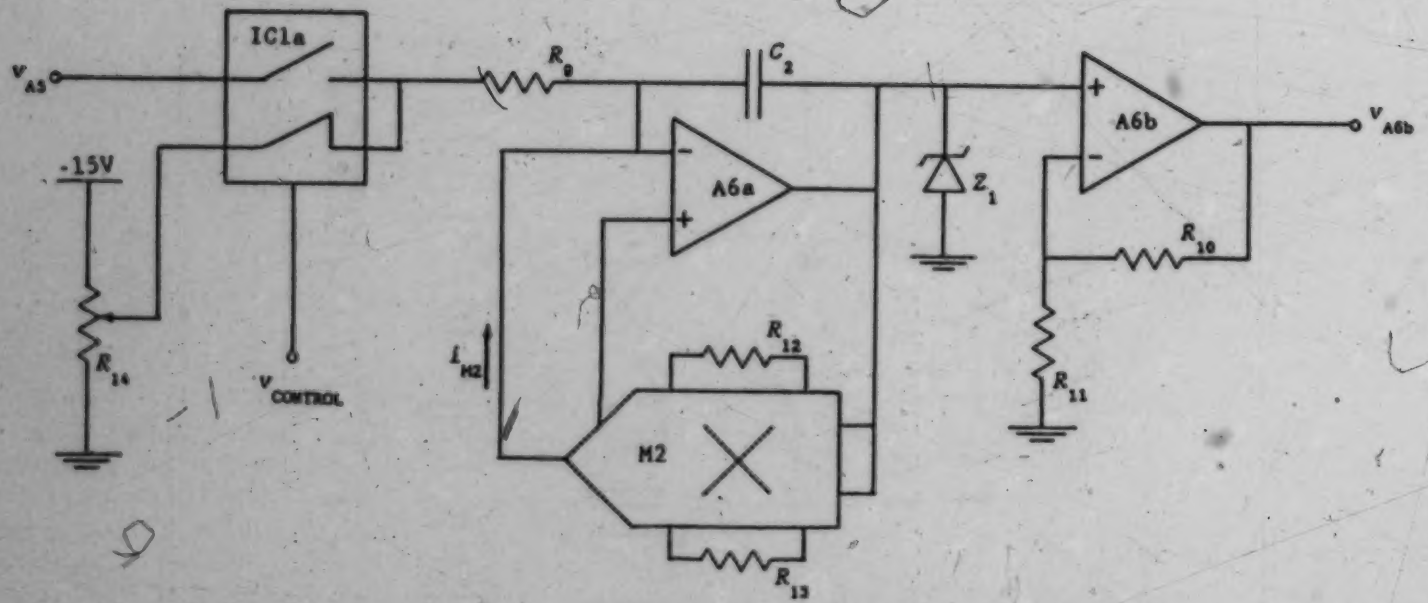

R_9 - 47kΩ R_{10} - 68 + 1.5kΩ R_{11} - 100kΩ R_{12} - 30kΩ R_{13} - 62kΩ
R_{14} - 10kΩ pot C_2 - 33pF Z_1 - 1N5242 IC1a - DG243 M2 - MC1594L
A6 - TL074C

FIG. 3.9 FAST AMPLITUDE CONTROL CIRCUITRY PART2

$$v_{A5} = -\frac{(2V_{MAX} + V_R - |v_1|)(|v_1| - V_R)}{30} \qquad (3.27).$$

The output of A5 is fed into a square root circuit (see Fig. 3.9). Taking a multiplier, tying the inputs together and putting it in the feedback path of an op-amp yields a circuit which performs the square root function. The output of M1 is a current given by (3.28).

$$i_{M1} = K_1 v_{A1a}^2 \qquad (3.28)$$

This current flows through R_1 and since the voltage at the inverting input of the op-amp is zero v_{A5} is given by

$$v_{A5} = -i_{M1} R_1 \qquad (3.29).$$

Combining (3.28) and (3.29) the output is given as

$$v_{A1a} = \sqrt{\frac{-v_{A5}}{K}} \qquad (3.30).$$

Note that since the square root function is defined for positive arguments, v_{A5} must be less than zero, otherwise the circuit will latch up. In other words, the feedback becomes positive and the op-amp saturates. To avoid this two things were done. The first was to include Z_1 which is an 11V zener diode. Should the output voltage swing negative then Z_1 will turn on preventing latch up. The other step taken was to ensure that the input is always negative. Consider the equation (3.27). The only time v_{A5} becomes positive is when $-V_R \leq v_1 \leq V_R$, which unfortunately happens twice every oscillation cycle. The purpose of the analog switch is to supply a negative voltage to the op-amp when the normal input goes positive. The control signal for the switch is derived in the later stages of the controller. It is simply the output of a comparator which tests this condition. Combining (3.27) and (3.30) the output expression for A1a

is given in (3.31).

$$V_{A1a} = \sqrt{\frac{(2V_{MAX} + V_R - |v_1|)(|v_1| - V_R)}{3}} \qquad (3.31)$$

The final stage is a non-inverting amplifier with a gain of $\sqrt{3}$ so that the final output expression is

$$V_{A1b} = \sqrt{(2V_{MAX} + V_R - |v_1|)(|v_1| - V_R)} \qquad (3.32)$$

It took a lot of circuitry just to get (3.32) and there is more to come.

The control law as stated in (2.58) can be expressed as a series of conditional tests. The testing can be done by comparators. The output of these tests, which can only have two possible outputs, can then be processed by logic circuits to determine when the control will switch. There are six conditions to test for. The final circuit is shown in Fig. 3.10.

It is known that $u(t)$ can have only two values: V_{MAX} or $-V_{MAX}$. Therefore, a logic variable, say Z, can be associated with $u(t)$ such that the following equation holds.

$$u(t) = \begin{cases} V_{MAX} & \text{when Z is true} \\ -V_{MAX} & \text{when Z is false} \end{cases} \qquad (3.33)$$

Now each of the six conditional tests can be associated with a logic variable, designated A through F, as described below.

A is true when $v_2 < \sqrt{(2V_{MAX} + V_R - |v_1|)(|v_1| - V_R)}$

B is true when $-v_2 > \sqrt{(2V_{MAX} + V_R - |v_1|)(|v_1| - V_R)}$

C is true when $v_1 < 0$

D is true when $|v_1| > V_R$

E is true when $v_2 > 0$

F is true when $v_o > 0$

Z can be related to the variables A-F by the following truth table.

A	B	C	D	E	F	Z
X	X	X	F	F	F	T
X	X	X	F	T	F	F
X	F	F	T	X	F	F
X	T	F	T	X	F	T
F	X	T	T	X	F	F
T	X	T	T	X	F	T
X	X	X	X	F	T	F
X	X	X	X	T	T	T

T = true
F = false
X = don't care

From the table is it easy to determine the expression for Z.

$$Z = EF + \check{D}\check{E}\check{F} + B\check{C}D\check{F} + ACD\check{F} \qquad (3.34)$$

The output of the logic circuitry then controls the state of the analog switch, which applies $\pm V_{MAX}$ according to the state of Z.

This section has covered the circuit design of the FAC. The circuits required to simulate the switching and the decision circuitry have been discussed. One can anticipate that errors in the circuit will largely be due to the square root circuit, especially when signals are small. Square root circuits aside, just the complexity of the control itself makes it prone to errors because of the amount of signal processing to be done. The complexity issue leads one to ponder whether any simplification would be possible. No doubt there is some simplification that is possible in terms of the reduction of

circuitry while still synthesizing the same control law. However, efforts applied to simplification might be better rewarded by finding a suitable approximation to the present control law.

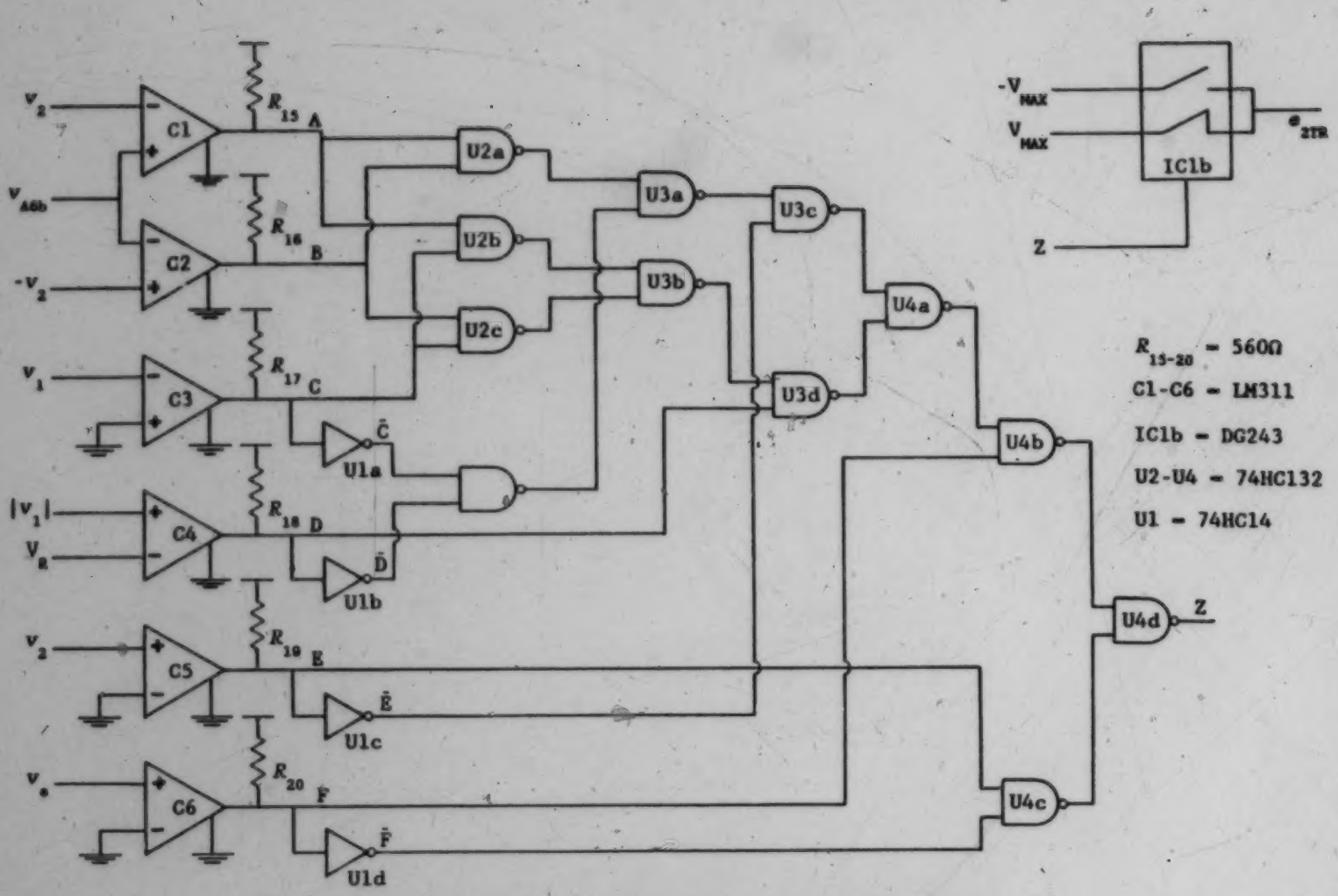

FIG. 3.10 FAST AMPLITUDE CONTROL CIRCUITRY PART3

3.2 TEST RESULTS

The test results are divided into two parts. The first part covers the distortion measurements that were made. This includes the sources of error that cause the distortion and derivation of equations to show the connection between the harmonic terms and the error sources. The results of the measurements are covered and methods to reduce the distortion are explained. The second part covers the transient response of the system. Most of the material discusses the phase plane portraits obtained.

Apart from the distortion and transient measurements made, some preliminary frequency measurements were made too. Consider the photographs in Fig. 3.11. Part a) shows the frequency of oscillation as 975 Hz, which is within the expected range explained in section 3.1.1. Part b) shows the phase difference between v_1 and v_2 as 88.6°, an error of 1.56%. Due to the success with which the tracking regulator worked it is believed that the phase shift is closer to 90° than the measurement shows and that the error is due to the measurement itself and not the circuit. Since there was no environmental chamber the temperature sensitivity could not be measured. Because the main concern was with the amplitude of the oscillator these were all the frequency measurements that were made.

3.2.1 Distortion Measurements

The dependence of the harmonics on the matching of the passive components in the tracking regulator can be learned by studying the ripple in the signal v_e. Theoretically, the signal v_e should be zero; however, because the poles of the oscillator have negative real parts

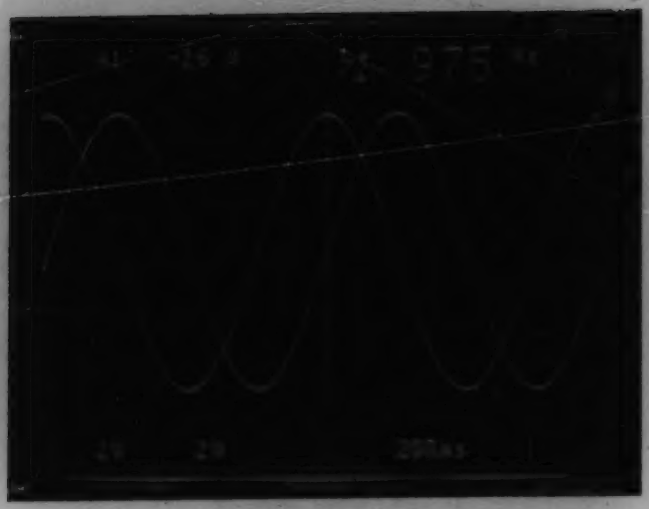

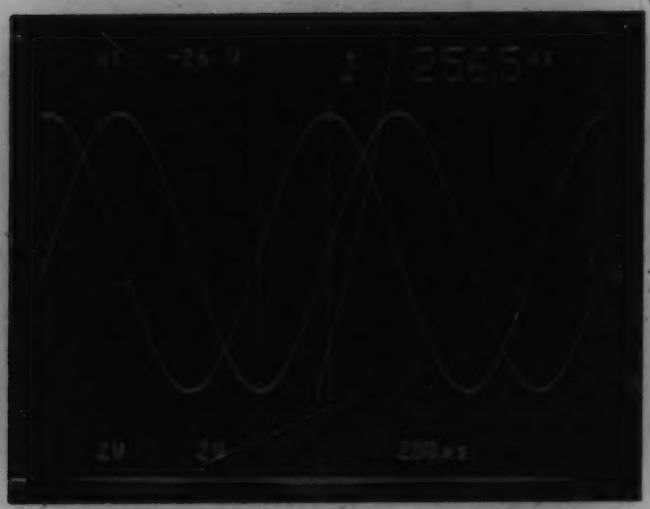

FIG. 3.11 FREQUENCY OF OSCILLATION AND PHASE DIFFERENCE

a small dc signal is expected. Any ac components in the signal result in harmonic components in the output signal. Therefore, the amount of ripple in v_e can be a relative measure of the distortion in the system. The resistances R_x, R_y and R_B (R_B determines I_B) initially were not matched. Since no matching was done the tolerance for K in the multipliers M2 and M3 in Fig. 3.6 was 15%. When the resistances were matched the resulting tolerance for K became 0.17% which resulted in a 77% reduction in the ripple voltage of v_e. Fig. 3.13a shows the ripple after matching. The resistors were matched with an ohmmeter. However, using thick film resistor arrays might prove better since they are not only tightly matched but track thermally as well. It is clear that tightly matched components in the circuits for M2 and M3 will do much to improve the total harmonic distortion.

The spectrum analyzer reveals what harmonic terms are present. The two dominant frequency terms are the first and second harmonics, which is not surprising; however, the second harmonic is larger than the first. Also the amplitude of the second harmonic frequency remains fixed while the first varies with time. It appears that the first term is related to noise and drift. At large amplitudes the third and fourth harmonic terms appear as well. Fig. 3.14 shows the frequency spectrum graph of the output v_1 at 10V. These, then, are the harmonic components that were measured. The sources of the distortion are considered next.

The analysis that follows is not meant to be a thorough distortion analysis but rather to show the connection between the error sources and the harmonic distortion terms they cause. The output of a multiplier including the op-amp has the following

expression [1]

$$V_0 = K(V_x + V_{iox} - V_{xoff})(V_y + V_{ioy} - V_{yoff}) + V_{oo} \qquad (3.35)$$

where V_x and V_y are the input signals, V_{iox} and V_{ioy} are the feedthrough offsets before nulling, V_{xoff} and V_{yoff} are the offset adjustment voltages and V_{oo} is the output offset. When the multiplier is operated as a squaring circuit the output is given as

$$V_0 = KV_x^2 + KV_x(\epsilon_x + \epsilon_y) + K\epsilon_x\epsilon_y + V_{oo} \qquad (3.36).$$

where $\epsilon_x = V_{iox} - V_{xoff}$ and $\epsilon_y = V_{ioy} - V_{yoff}$. The output of M1 will be assumed ideal since it is only a dc signal and does not contribute to the distortion terms. The same argument applies to the terms $K\epsilon_x\epsilon_y$ and V_{oo} in (3.36) when it is applied to M2 and M3. Therefore, the output of A2 can now be given as

$$v_{A2} = KV_R^2 - \left\{K_{M2}v_1^2 + K_{M2}v_1(\epsilon_{X2} + \epsilon_{Y2}) + K_{M3}v_2^2 + K_{M3}v_2(\epsilon_{X3} + \epsilon_{Y3})\right\} \qquad (3.37)$$

Let $v_F = \epsilon_{X2} + \epsilon_{Y2} = \epsilon_{X3} + \epsilon_{Y3}$ since these represent small signals and all are due to feedthrough in the multpliers. To simplify matters even further let $K = (K_{M2} + K_{M3})/2$ and $\Delta K = (K_{M2} - K_{M3})/2$. Applying some algebra and assuming that $v_o = av_{A2}$ the expression for v_o becomes

$$v_o = aK\left\{(V_R^2 - [v_1^2 + v_2^2]) - v_F(v_1 + v_2) + \frac{\Delta K}{K}[(v_1^2 - v_2^2) + v_F(v_1 - v_2)]\right\} \qquad (3.38)$$

Ignoring the final term of (3.38) and assuming that M4 and M5 are ideal the expressions for e_{1SS} and e_{2SS} are given by

$$e_{1SS} = -aK^2v_1\left\{(V_R^2 - [v_1^2 + v_2^2]) - v_F(v_1 + v_2) + \frac{\Delta K}{K}(v_1^2 - v_2^2)\right\} \qquad (3.39)$$

$$e_{2SS} = -aK^2v_2\left\{(V_R^2 - [v_1^2 + v_2^2]) - v_F(v_1 + v_2) + \frac{\Delta K}{K}(v_1^2 - v_2^2)\right\} \qquad (3.40).$$

Consider e_{1SS} and let $v_1 = V_R \sin \beta t$ and $v_2 = V_R \cos \beta t$. The resulting e_{1SS} is

$$e_{1SS} = \frac{aK^2V_R^2}{2}\left\{v_p - V_R\frac{\Delta K}{K}\sin \beta t - \sqrt{2}\, v_p \cos(2\beta t + \frac{\pi}{4}) + V_R\frac{\Delta K}{K}\sin 3\beta t\right\} \qquad (3.41)$$

Equation (3.41) shows that the distortion terms are a function of the amplitude and this can be seen in the graph of Fig. 3.12. Equation (3.41) also shows that the first harmonic is a function of the feedthrough voltage in M2 and M3. This would explain the dependence on drift and noise. Finally, (3.41) indicates that the second harmonic is dependent on the mismatch in K. It appears that the mismatch in K is larger than the 0.2% which was indicated before. This is probably due to differences in M2 and M3 which has not been accounted for. Although (3.41) does not correctly show the values of the coefficients of the harmonic terms, it does illustrate how the harmonic terms arise due to the error sources in the magnitude detector circuit consisting of M2 and M3 in Fig 3.6.

If the THD figures shown in Fig. 3.12 are not acceptable then other ways must be considered to reduce the distortion. Two approaches will be discussed that reduce the distortion without changing the topology of the circuit. The most obvious approach is to filter out the ripple in v_e. The second curve in the graph of Fig. 3.12 illustrates what happens when a filter is added. This filter is the circuit in the dashed box shown in Fig. 3.6 with a time constant τ = 10 msecs. At an amplitude of 10V the THD drops to -77.5 dB (0.013%). In fact Fig. 3.13 shows the control voltages e_{1SS} and

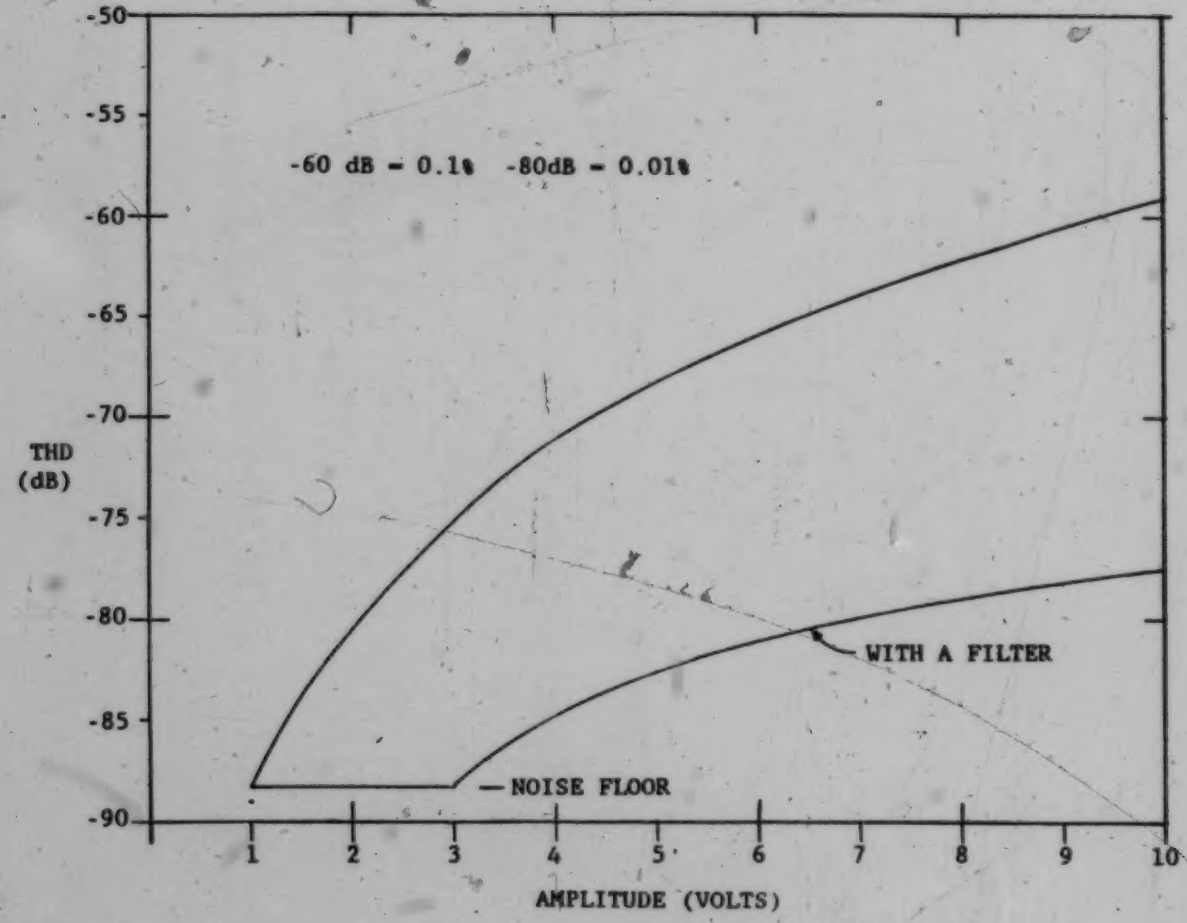

FIG. 3.12 DISTORTION AS A FUNCTION OF AMPLITUDE

a) WITHOUT A FILTER

b) WITH A FILTER

FIG. 3.13 THE RIPPLE VOLTAGE PRESENT IN THE CONTROL SIGNALS

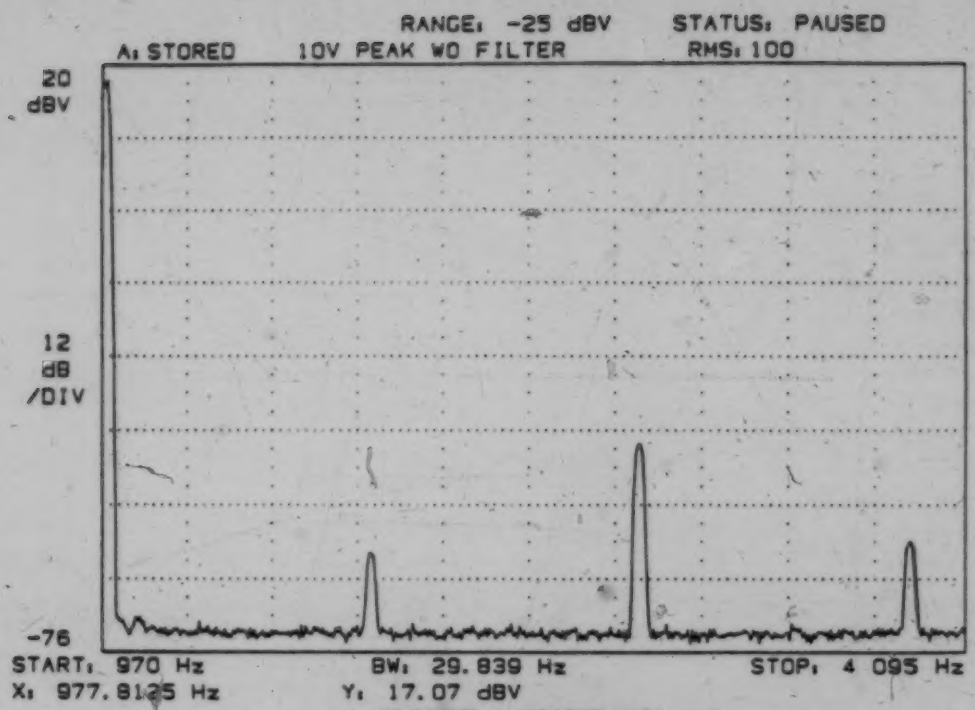

a) WITHOUT A FILTER AND $a=1$

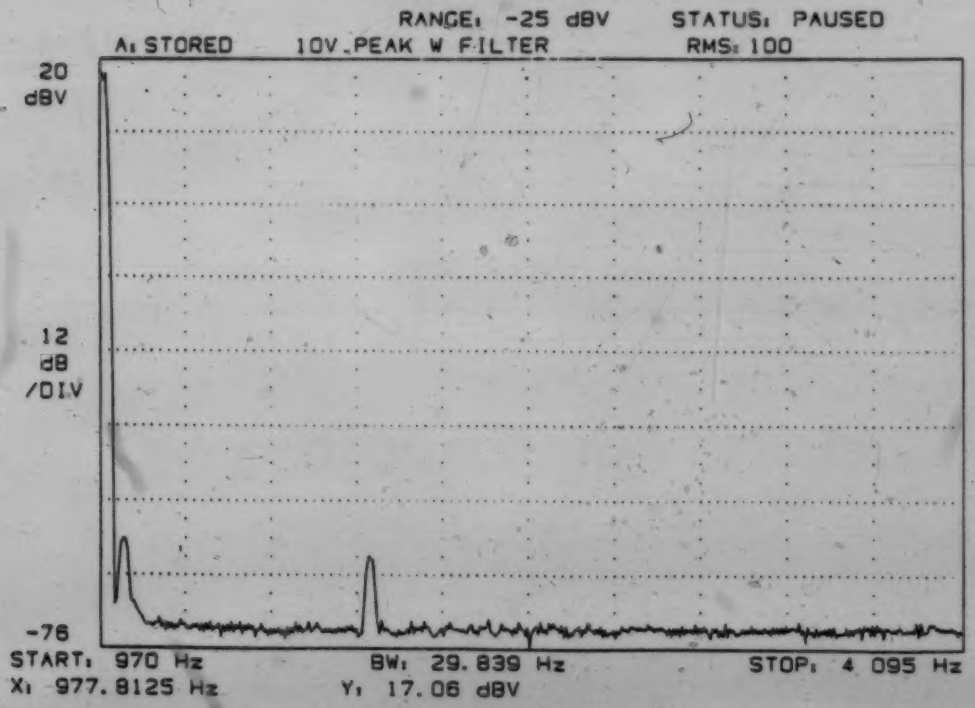

b) WITH A FILTER AND $a=1$

FIG. 3.14 FREQUENCY SPECTRUM FOR AN AMPLITUDE [illegible]V

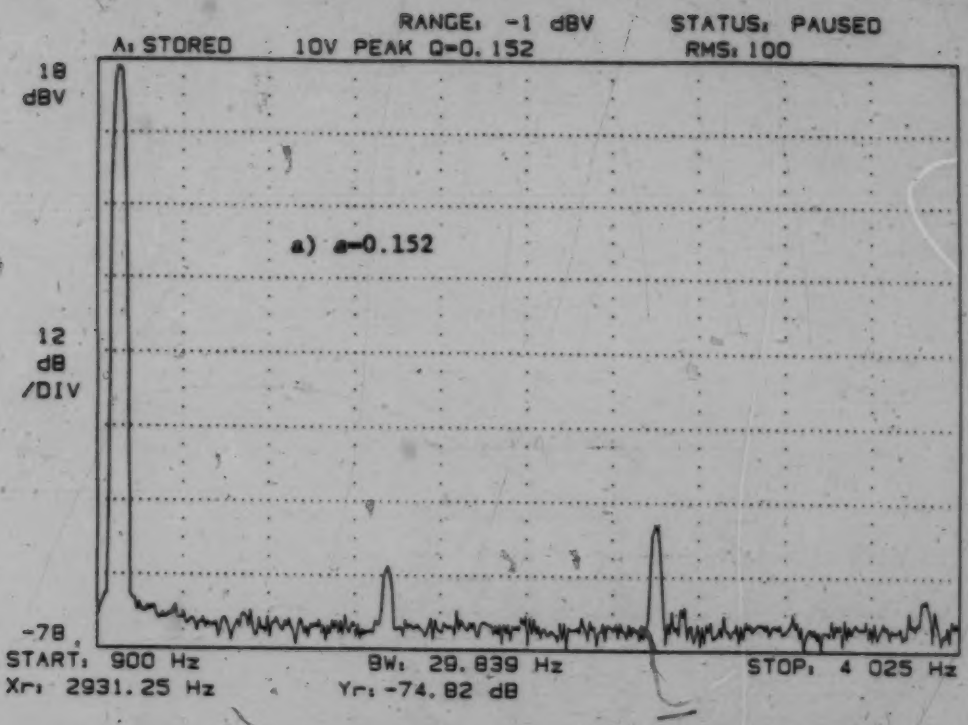

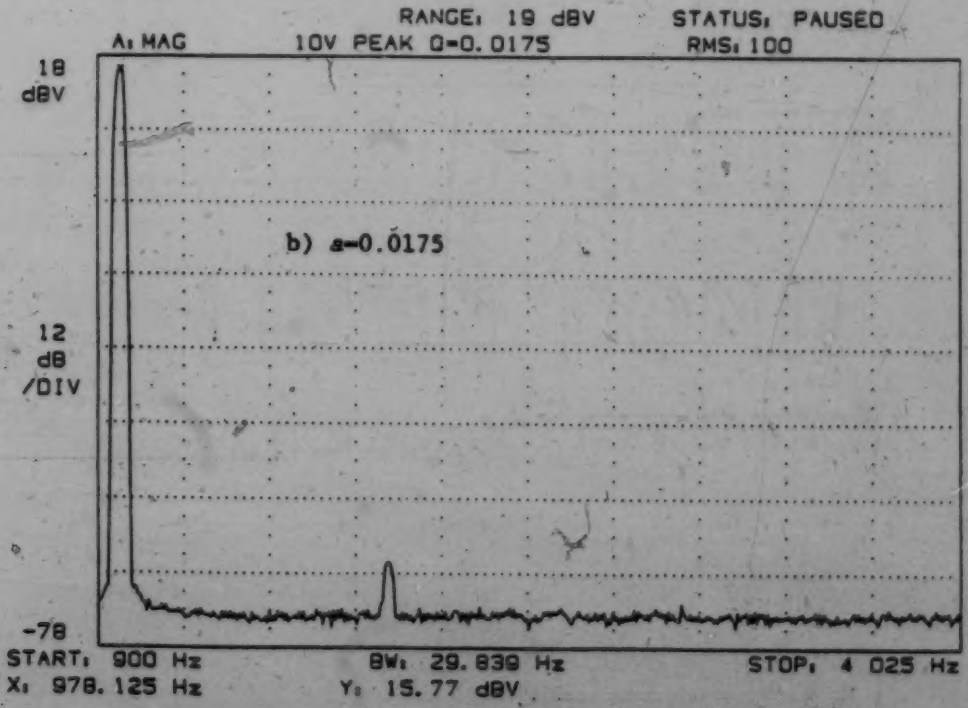

FIG. 3.15 FREQUENCY SPECTRUM FOR AN AMPLITUDE OF 10V

e_{ss} before and after filtering. The filter was one attempt at decreasing the distortion in the signal by smoothing the ripple in v_e.

Another approach was to replace the filter with a voltage divider. The network chosen was such that the constant a, which appears in the control equations (3.39) and (3.40), was 0.152. The result was similar to the filter. The THD was -75 dB (0.018%) at 10V. However, since the dc component of v_e is also reduced a change in the amplitude results. The change in amplitude is rather small. For a nominal 10V amplitude the divider causes it to drop to 9.90V, a change of only 1%. The voltage divider has the advantage of not introducing any delay into the feedback path. When a was further reduced to 0.0175 the THD became -79.25 dB (0.011%). However, the amplitude dropped to 8.7V from 10V. So it appears that further attenuation of v_e does not pay off. With either the filter in place or a set to 0.0175 it was the first harmonic that was dominant rather than the second, which indicates that there was another source of distortion from those already discussed. The filter spectrum plots are shown in Figs. 3.14 and 3.15. These plots cover the situations discussed. It was not until after these measurements had been made that the other error source was finally discovered.

The cause of the first harmonic term which was only apparent when the filter was in place was due to another mismatch problem, this time between the multipliers M4 and M5. Again the problem is the mismatch in the scaling factors. However, the problem was easily remedied by adjusting the scaling factor of one of the multipliers.

How the mismatch in M4 and M5 causes the distortion term can be determined by considering the expressions for the two control signals

e_{1SS} and e_{2SS} where the signal v_e is assumed ideal. This asumption can be made since the signal v_e is either filtered or attenuated by the voltage divider to such an extent that distortion due to M2 and M3 is small in comparison to M4 and M5. Indeed

$$e_{1SS} = -aKK_4(V_R^2 - (v_1^2 + v_2^2))v_1 \qquad (3.42)$$

$$e_{2SS} = -aKK_5(V_R^2 - (v_1^2 + v_2^2))v_2 \qquad (3.43)$$

Let

$$K = \frac{K_4 + K_5}{2} \qquad \Delta K = \frac{K_4 - K_5}{2} \qquad (3.44)$$

The differential equations which describe the oscillator are given by (3.45) and (3.46) when (3.42) and (3.43) are used for the control signals.

$$\dot{v}_1 = [\beta aKK_4(V_R^2 - [v_1^2 + v_2^2])]v_1 + \beta v_2 \qquad (3.45)$$

$$\dot{v}_2 = -\beta v_1 + [\beta aKK_5(V_R^2 - [v_1^2 + v_2^2])]v_2 \qquad (3.46)$$

Now let

$$\gamma = \frac{\gamma_1 + \gamma_2}{2} \qquad \Delta\gamma = \frac{\gamma_1 - \gamma_2}{2} \qquad (3.47)$$

where

$$\gamma_1 = [\beta aKK_4(V_R^2 - [v_1^2 + v_2^2])] \quad \text{and} \quad \gamma_2 = [\beta aKK_5(V_R^2 - [v_1^2 + v_2^2])].$$

Using the definitions of (3.44) and (3.47) the following relations are true.

$$\gamma = \beta aK^2(V_R^2 - [v_1^2 + v_2^2]) \qquad (3.48)$$

$$\gamma_1 = \gamma(1 - \Delta K/K) \qquad \gamma_2 = \gamma(1 + \Delta K/K) \qquad (3.49)$$

$$\Delta\gamma = \gamma(\Delta K/K) \qquad (3.50)$$

The differential system can now be re-stated as

$$\dot{v}_1 = \gamma(1 - \Delta K/K)v_1 + \beta v_2 \qquad (3.51)$$

$$\dot{v}_2 = -\beta v_1 + \gamma(1 + \Delta K/K)v_2 \qquad (3.52)$$

The key point is that the mismatch in K_4 and K_5 creates a mismatch in

the term γ and it is this mismatch that strangely enough causes the distortion term. The effect can be better understood when the differential system of (3.51) and (3.52) is transformed into polar coordinates. The resulting system is given now as

$$\dot{r} = r\gamma(1 + (\Delta K/K) \cos 2\theta) \tag{3.53}$$

$$\dot{\theta} = \gamma(\Delta K/K) \sin 2\theta + \beta \tag{3.54}$$

$$\gamma = \beta a K^2 (V_R^2 - r^2) \tag{3.55}.$$

When the system is ideal the two equations in (3.53) and (3.54) decouple and can then be solved separately. It is the coupling between the phase and the amplitude that causes the distortion and this is how the mismatch in M4 and M5 causes the additional first harmonic term.

3.2.2 Transient Response

The transient response is a function of the change in amplitude and when the signal to change with respect to the period of oscillation occurs. This makes measurements difficult. A full set of responses would have required a special triggering circuit. What was done was to photograph some representative responses (see figs. 3.16 to 3.20). To begin, consider the oscilloscope photographs in Figs. 3.16 and 3.17. Figure 3.16 shows the rise time from a 2V amplitude to 10V, with 3.16b showing an expanded version of the transient. As can be seen in the picture the rise time is about 200μsecs. It should be noted that the photo in 3.16b depicts a different starting point than in 3.16a. What is demonstrated in these photographs is that the control never switches and that the transient is always less than the period of oscillation. This is the fastest transient ever recorded.

Much the same applies for the fall time shown in the photographs in Fig 3.17. The key difference here is that the control switches once. This is the most that the control will ever switch. Under certain conditions it may not switch at all.

The photos in Fig.3.16 and 3.17 do not tell the whole story. In Figs. 3.18 and 3.19 v_1 and v_2 have been plotted against each other to create the phase plane portraits. It is now easy to see that the FAC confirms the phase plane plots done in chapter 2. In each photo both the amplitude rise and fall are shown. Fig 3.18a shows the situation where the control does not switch during the amplitude decrease. Note that the trajectory is traced in the clockwise direction. The transient rise is shown in the upper part of the trace and the fall in the bottom part of the trace. In Fig. 3.18b one can see that control switches during the fall in amplitude. In Fig 3.19 a slightly different situation occurs. The reason for the double trace is due to the difference in frequency between the oscillator and the signal generator and is not a result of the circuit. One can immediately see the overshoot here. There are several reasons for the overshoot. The first reason is a gain error in the FAC caused by the square root circuit which in turn causes the switching curve to be out of place. The overshoot can also be affected by the width of the window in the DMC. Finally, the tracking regulator and the FAC do not see the same reference signal. This is due offset errors in the squaring circuit of the tracking regulator. To correct or minimize these errors would require careful measurements and a way of measuring the actual switching curve, something which was not available. However, the circuit still produces very fast responses, with the worst case

transient being less than half the period of oscillation.

Figure 3.20 illustrates what happens when the tracking regulator is shut off and the FAC is allowed to operate during the steady state. The FAC simply chatters and causes the ripple seen in the photo. Note that v_1 still appears as a smooth sine wave since it is indirectly controlled. In other words, v_1 is v_2 filtered due to the integrator.

In this chapter the implementation of the control systems has been looked at. The shortcomings of the circuits have been studied with special attention paid to distortion and settling time. The performance of the tracking regulator can make modest claims in terms of the THD obtained whereas the FAC has the fastest time claimed in the research literature. However, the circuits are not in their final form and with the insights gained it should be possible to derive improved circuits with better performances.

a)

b)

FIG. 3.16 AMPLITUDE RISE TIME

a)

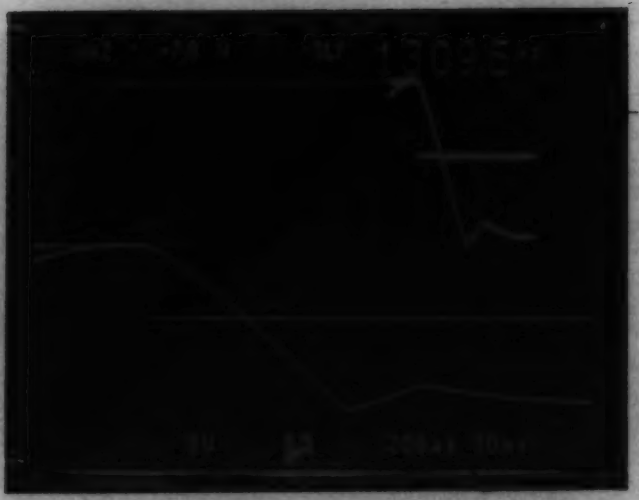

b)

FIG. 3.17 AMPLITUDE FALL TIME

a)

b)

FIG. 3.18 PHASE PLANE PORTRAITS

FIG. 3.19 PHASE PLANE TRANSITION

FIG. 3.20 FAC OPERATION ON STEADY STATE

4.0 SUGGESTIONS FOR FURTHER RESEARCH

It can be said with some confidence that the control systems derived in chapter 2 are complete. The same is not true with their circuit implementation. The design of the circuits took the most direct approach. The tracking regulator needs to be redesigned and optimized in order to reduce the distortion that it introduces as well as overcome the other problems that were discussed. The FAC needs to be simplified. The first step is to attempt to simplifiy the control law approximation. After that the circuit requires simplification. The FAC should also be disabled during steady state to reduce noise caused by its switching of signals when it operates. Means to better measure its performance are needed so that the sources of error can be determined. Investigation of these areas would go a long way to putting the oscillator circuit in its final form. Another area to research is different performance criterion. It would be interesting to investigate what kind of control would result if a sensitivity measure was added to the tracking regulator. The measure would be the oscillator's state variables' sensitivity to the controls. The intent is to reduce the distortion by minimizing the sensitivity. Another criterion to try is one which combines the tracking error and time. This would eliminate the need for two separate control systems. Such a performance index would never be as fast as the one already studied but it might have less complexity. Actually, the choice of criterion becomes limitless and will ultimately depend on the oscillator's application.

One of the applications of the oscillator is as part of a function generator. However, it is not complete without the ability to change the frequency of oscillation. Applying optimal control theory to the design of a frequency controller might have interesting results. For example, minimizing the frequency transients would result in a fast frequency controller, in other words, a phase locked loop with fast frequency lock. With both frequency and amplitude control applied the resulting oscillator would be quite impressive.

The final area of further research is the fabrication of the circuit into a chip. The circuit's appeal would probably increase if a digital input was added for the amplitude and the frequency as well as a method for automatic calibration. Then the circuit could be used by automated equipment and the computer could compensate for temperature and aging effects. The best result of this thesis was to raise more questions than answers.

4.1 CONCLUSION

Optimal control theory was a useful tool in the design of the control system, particularly the fast amplitude controller. Without it the FAC never would have been conceived. The performance of the circuit speaks for itself. However, the major drawback is that the results of optimal control theory are such that they do not lend themselves readily to circuit synthesis, largely due to the open loop nature of the solutions. Ultimately, a mathematical "trick" is required to obtain the resulting control in closed loop form; the use of geometric methods applied to the phase plane in the solution of the time optimal control problem can be cited as an example. If the problem had been third order instead of second there would have been little hope of obtaining any useful results from the solution. However, all that has really taken place is a shift in effort from the circuit design to applying some ingenuity in finding a closed loop solution to the control. Regardless of the view one takes, optimal control theory, as applied to circuit design, is something that has been overlooked by engineers. Despite many drawbacks it remains a valid design tool.

The design method used, as presented in this thesis, has differed from the traditional approach. It has been synthetic instead of analytic and systematic rather than intuitive. It also differs in that the model used a state variable description instead of an input-output transfer function. This was in part due to the nonlinear nature of the system but more so because of the use of optimal control theory. Whether this approach is any better depends on whether performance outweighs other factors, especially cost. In a commercial

design cost may be the major design objective in which case a short development time and simplicity in the design may force a more intuitive approach. However, a systematic method is amenable to implementation into a CAD environment. As well, fabrication of the circuit in silicon may negate the need for simplicity - consider the history of microprocessor chips. Regardless, the approach has merit since it produces a circuit that works and works well.

BIBLIOGRAPHY

References for Chapter One

[1]. B. J. Skehan, "Design of an Amplitude-Stable Sine-Wave Oscillator", *IEEE J. Solid-State Circuits*, vol. SC-3, pp. 312-315, Sept. 1968.

[2]. P. W. Van Der Walt, "A Wien-Bridge Oscillator with High-Amplitude Stabilty", *IEEE Trans. Instrumentation & Measurement*, vol. IM-30, no. 4, Dec. 1981.

[3] D. Meyer-Ebrecht, "Fast Amplitude Control of a Harmonic Oscillator", *IEEE Proc.*, vol. 60, p. 736, 1972.

[4]. D. Meyer-Ebrecht, "Schnelle Amplitudenregelung Harmonischer Oscillatoren", *Philips Res. Rep.*, vol. 6, pp. 1-85, 1974.

[5]. E. Vannerson and K. C. Smith, "A low-distortion oscillator with fast amplitude stabilization", *Int. J. Electronics*, vol. 39, pp. 465-472, 1975.

[6]. W. B. Mikhael and S. Tu, "Continuous and Switched-Capacitor Multiphase Oscillators", *IEEE Trans. Circuits Syst.*, vol. CAS-31, pp. 280-292, 1984.

[7]. J. Pahor, J. Fetteich and M. Tavzes, "A harmonic oscillator with low harmonic distortion and stable amplitude", *Int. J. Electronics*, vol. 37, pp. 765-768, 1974.

[8]. N. Vannai and L. Pap, "*RC*-oscillator with extremely low harmonic distortion," *Period. Polytechn. (Hungary) Elect. Eng.*, vol. 24, pp.59-65, 1980.

[9]. I. M. Filanovsky, "A Wien bridge *RC* oscillator with fast amplitude control", *Int. J. Electronics*, vol. 58, pp. 817-826, 1985.

[10]. I. M. Filanovsky, V. A. Piskarev and K. A. Stromsmoe, "On the fast amplitude control in *RC*-oscillators", *Proc. IEEE Int. Symp. Circuits Syst.*, (Rome), May 1982, pp. 819-822.

[11]. E. Vannerson and K. C. Smith, "Fast Amplitude Stabilization of an *RC* Oscillator", *IEEE J. Solid-State Circuits*, vol. SC-9, pp. 176-179, Aug. 1974.

[12]. I. M. Filanovsky and G. J. Fortier, "Fast amplitude control in Twin-T *RC*-oscillators", *Electronics Letters*, vol. 21, pp. 791-792, 1985.

References for Chapter Two

[13]. Andrew P. Sage, *Optimum Systems Control*, Prentice Hall Inc., Englewood Cliffs, N.J., 1968.

[14]. Michael Athans and Peter L. Falb, *Optimal Control: An Introduction to the Theory and Its Applications*, McGraw-Hill, New York, 1966.

[15]. L. S. Pontryagin, V. G. Boltyanskii, R. V. Gamkrelidze, and E. F. Mishchenko, *The Mathematical Theory of Optimal Processes*, John Wiley & Sons, New York, 1962.

[16]. Jack Macki and Aaron Strauss, *Introduction to Optimal Control Theory*, Springer-Verlag, New York, 1982.

[17]. M. Herpy, *Analog Integrated Circuits*, John Wiley & Sons, New York, 1980.

[18]. M. Vidyasagar, *Nonlinear Systems Analysis*, Prentice-Hall Inc., Englewood Cliffs N.J., 1978.

References for Chapter Three

[19]. *Linear and Interface Integrated Circuits Data Book*, Motorola Inc., 1985.

[20]. *Linear Circuits Data Book*, Texas Instruments, 1984.

[21]. *Linear and Conversion Products*, Precision Monolithics, 1986.

[22]. *Analog Switch & IC Product Data Book*, Siliconix Inc., 1982.